Journal of Sound and Vibration (1999) **221**(1), 85–116
Article No. jsvi.1998.1989, available online at http://www.idealibrary.com on IDEAL

ACTIVE CANCELLATION OF ACOUSTIC PRESSURE AND PARTICLE VELOCITY IN THE NEAR FIELD OF A SOURCE

J. GARCÍA-BONITO

Institute for Applied Automotive Research (*IDIADA*), *L'Alborner*, *E*-43710 *Santa Oliva*, *Tarragona*, *Spain*

AND

S. J. ELLIOTT

ISVR, *University of Southampton*, *Southampton SO*17 1*BJ*, *England*

(*Received* 14 *July* 1997, *and in final form* 24 *September* 1998)

In a local active noise control system the pressure signal from a single microphone is usually taken as the error signal and cancelled by the action of a secondary source to create a zone of quiet. In this paper it is shown that the strategy of cancelling the acoustic pressure and a component of the particle velocity at a point in the near field of a secondary source considerably improves the acoustic performance of a local active noise control system with respect to the case in which only the acoustic pressure is cancelled. It is also shown that in the near field of a secondary source the active cancellation of the acoustic pressure and the particle velocity component due to only the secondary source produces similar near field zones of quiet to those obtained when the acoustic pressure and the total particle velocity component are cancelled instead. This suggests that an array of two loudspeakers having a fixed gain and phase relationship could be used as the single secondary source. The acoustic performance of a secondary source array formed by two loudspeakers is theoretically studied when the acoustic pressure and the secondary particle velocity component is cancelled at a point in its near field with and without a diffracting head present. The results show that this sort of secondary source array can produce larger near field zones of quiet than a conventional loudspeaker cancelling the acoustic pressure only. Finally, the acoustic performance of such a secondary source array in a local active noise control system with a virtual microphone arrangement that projects the zone of quiet further away from the secondary source than the position of the physical microphone is also studied. For this sort of arrangement, it will be shown that the cancellation of the pressure and the secondary particle velocity at two different points in the near field of the secondary source gives better performance than the cancellation of both acoustic magnitudes at the same field point.

1. INTRODUCTION

In a conventional local active noise control system, the pressure signal from a single cancellation microphone, taken as the error signal, is cancelled by the action of the secondary source that creates the zone of quiet. Control of the pressure has

0022–460X/99/110085 + 32 $30.00/0

also been the most widely studied strategy even for multi-channel active noise control systems in which the sum of the squares of the signals from an array of microphones is minimized by adjusting the inputs to an array of loudspeakers.

Recently, it has been shown that the cancellation not only of the acoustic pressure but also of its spatial gradient in a particular direction, which is proportional to the acoustic particle velocity component, provides a considerable improvement in the acoustic performance of certain noise control arrangements [1]. Miyoshi *et al*. [2] have used the strategy of cancellation of pressure at multiple microphones in their simulations for a multi-channel active control system and showed that this approach produces larger zones of quiet. Ise [3] has discussed the effect of cancelling the pressure at two closely-spaced microphones in order to implement what he calls ''active impedance control''.

The work described in this paper explores the advantages and disadvantages of controlling the acoustic pressure and the particle velocity component at a single or at two different points in the near field of a secondary source to generate a zone of quiet in a diffuse sound field. It will be shown that this control strategy offers a way of increasing the size of the achievable zone of quiet in the direction of the particle velocity component which is set to zero. In particular, it will be shown that the cancellation of acoustic pressure and *total* particle velocity component allows us to obtain broader zones of quiet regardless of the nature of the primary acoustic field.

Also explored is the effect that controlling the pressure and the secondary acoustic particle velocity component has on the zones of quiet created in the near field of a secondary source composed of an array of loudspeakers. It will be shown that when only the acoustic pressure and the *secondary* particle velocity is cancelled at one point, the local control system may need only one error microphone in order to generate zones of quite of similar size to those obtained when the acoustic pressure and the *total* particle velocity component are cancelled.

2. ACTIVE CANCELLATION OF ACOUSTIC PRESSURE AND TOTAL PARTICLE VELOCITY COMPONENT IN THE NEAR FIELD OF A SECONDARY SOURCE

This section is concerned with investigating the effect of simultaneously cancelling the acoustic pressure and the *total* particle velocity component in the near field of a secondary source. In order to simplify the simulations, the secondary source has been modelled as an array of two independent monopoles whose source strengths are adjusted so that the acoustic pressure and total particle velocity component in the x-direction at an error sensor location are cancelled. Figure 1 shows the assumed geometry, where it is shown that the two monopoles are a distance d apart in the x-direction and the cancellation sensor is located at $(x, y) = (L, 0)$. The total pressure and particle velocity in the x-direction at a field point (r, θ) can be expressed as

$$p_T(r, \theta) = p_p(r, \theta) + q_{s1} Z_{ps1}(r, \theta) + q_{s2} Z_{ps2}(r, \theta), \tag{1a}$$

$$u_{xT}(r, \theta) = u_{xp}(r, \theta) + q_{s1} T_{u_x s1}(r, \theta) + q_{s2} T_{u_x s2}(r, \theta), \tag{1b}$$

where q_{s1}, q_{s2} are the monopole secondary source strengths; $Z_{ps1}(r, \theta)$, $Z_{ps2}(r, \theta)$, the acoustic transfer impedances from monopole 1 and 2 to the field point (r, θ), respectively, and $T_{u_x s1}(r, \theta)$, $T_{u_x s2}(r, \theta)$ are the acoustic transfer functions that relate the strength of each monopole with their respective acoustic particle velocity in the x-direction. p_p and u_{xp} denote the acoustic pressure and the particle velocity component in the x-direction due to the primary sound field respectively. The expressions for $Z_{ps1}(r, \theta)$, $Z_{ps2}(r, \theta)$, $T_{u_x s1}(r, \theta)$ and $T_{u_x s2}(r, \theta)$ are given by

$$Z_{ps1}(r, \theta) = \frac{j\omega\rho_o}{4\pi r_1} e^{-jkr_1}, \qquad Z_{ps2}(r, \theta) = \frac{j\omega\rho_o}{4\pi r_2} e^{-jkr_2}, \tag{2a}$$

$$T_{u_x s1}(r, \theta) = \frac{e^{-jkr_1}}{4\pi} \cdot \left(\frac{jk}{r_1} + \frac{1}{r_1^2}\right) \cos(\theta_1), \qquad T_{u_x s2}(r, \theta) = \frac{e^{-jkr_2}}{4\pi} \cdot \left(\frac{jk}{r_2} + \frac{1}{r_2^2}\right) \cos(\theta_2), \tag{2b}$$

where

$$r_1 = \sqrt{(d/2)^2 + r^2 - rd\cos(\theta)}, \qquad r_2 = \sqrt{(d/2)^2 + r^2 + rd\cos(\theta)},$$

$$\cos(\theta_1) = \sqrt{1 - \left(\frac{r}{r_1}\sin(\theta)\right)^2}, \qquad \cos(\theta_2) = \sqrt{1 - \left(\frac{r}{r_2}\sin(\theta)\right)^2}.$$

Equations (1a) and (1b) can be expressed in matrix form as

$$\begin{pmatrix} p_T \\ u_{xT} \end{pmatrix} = \begin{pmatrix} p_p \\ u_{xp} \end{pmatrix} + \begin{pmatrix} Z_{ps1} & Z_{ps2} \\ T_{u_x s1} & T_{u_x s2} \end{pmatrix} \begin{pmatrix} q_{s1} \\ q_{s2} \end{pmatrix}. \tag{3}$$

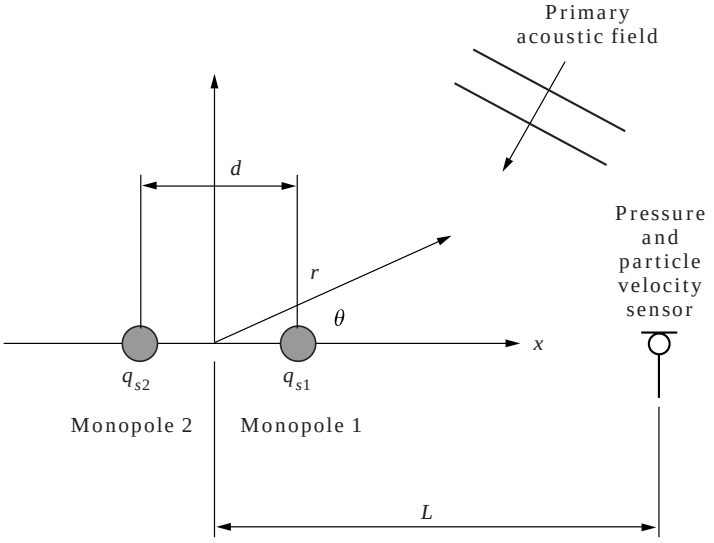

Figure 1. Geometry for the simulation of active noise control of acoustic pressure and particle velocity component.

In order to cancel the acoustic pressure and the total particle velocity component along the x-direction at a point of co-ordinates $(r, \theta) = (L, 0)$, q_{s1} and q_{s2} have to take the respective values given by the matrix equation

$$\begin{pmatrix} q_{s1o} \\ q_{s2o} \end{pmatrix} = -\begin{pmatrix} Z_{ps1} & Z_{ps2} \\ T_{u_x s1} & T_{u_x s2} \end{pmatrix}^{-1}_{(L,0)} \begin{pmatrix} p_p \\ u_{xp} \end{pmatrix}_{(L,0)}, \tag{4}$$

where the sub-index $(L, 0)$ denotes that the elements in the matrix and vector correspond to the position of co-ordinates $(L, 0)$. By substituting the values of q_{s1o} and q_{s2o} obtained from equation (4) into equation (1a), the controlled acoustic pressure field can be calculated and compared with the primary acoustic field to yield the produced zone of quiet.

3. NEAR FIELD ZONES OF QUIET AFTER CANCELLATION OF ACOUSTIC PRESSURE AND TOTAL PARTICLE VELOCITY COMPONENT

In this section the calculated zones of quiet created by the two monopole secondary source array of Figure 1 seeking to cancel the pressure and total particle velocity component in the x-direction at a point near the source array [4] are presented.

Figure 2 (left column) shows the calculated zones of quiet produced by the source arrangement of Figure 1, for $kL = 0{\cdot}5$, when the primary acoustic field is uniform on the x–y plane, i.e., a plane wave propagating in the z-direction, and the pressure and the total particle velocity component along the x-direction are cancelled at the error sensor position (represented as "+" in the contour plots). The two-monopole secondary sources are shown as dots at $(\pm d/2, 0)$. These results can be compared with those shown in the right column of the same figure which depict the zones of quiet that would be obtained with a single-monopole secondary source at (0, 0) cancelling the pressure only at the same error sensor position. One can observe that, for this case, the cancellation of pressure and total particle velocity considerably increases the extension of the zone of quiet with respect to the strategy of simply cancelling the pressure. The frequency studied corresponds to $kL = 0{\cdot}5$, where L is the distance between the error sensor, which now is assumed to measure acoustic pressure and particle velocity, and the mid-point between the two monopoles. For the sake of simplicity, the distance between the monopoles, d, has been taken equal to L. In this calculation, the strengths of the two monopoles were adjusted to cancel the acoustic pressure and the total particle velocity component along the x-direction. Each contour plot, in both left and right columns, is accompanied by a plot of the mean square pressure associated to the primary acoustic field (dashed line), secondary acoustic field (dash-dot line) and total acoustic field (dotted line) along the x-direction after control. The independent representation of these three acoustic fields reveals that in order to cancel the pressure and particle velocity, the monopole located further away from the error sensor (monopole 2) has to be driven considerably harder than the one at the closer position (monopole 1). This point will be studied in more detail in section 6. One can also observe that the increase in the "diameter" of the

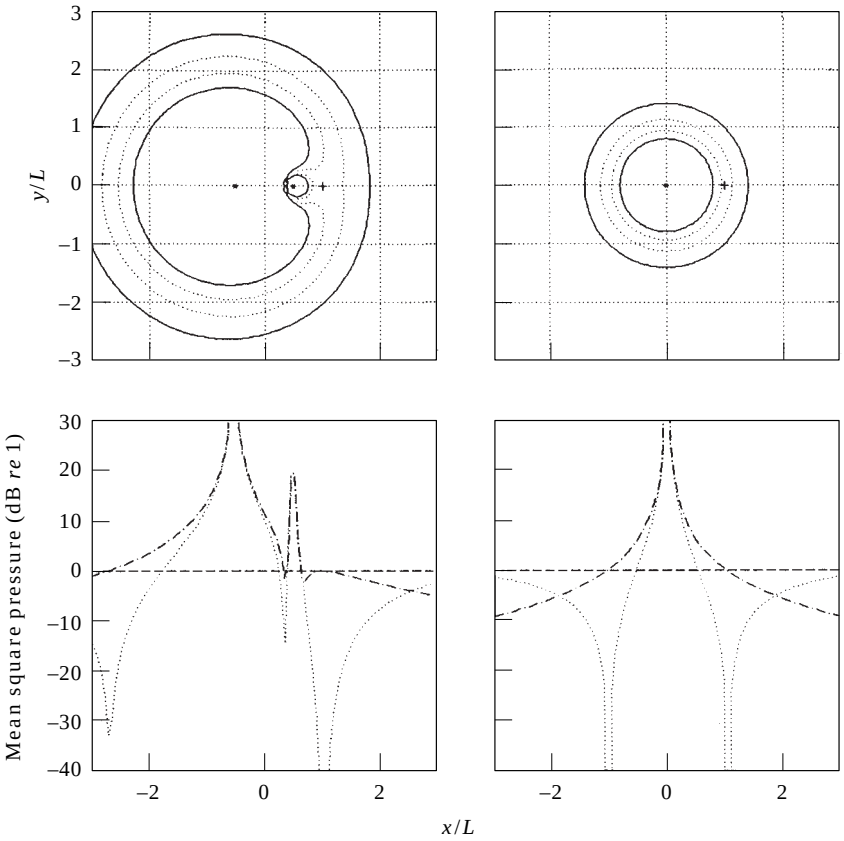

Figure 2. Left column: the zone of quiet created by a two-monopole secondary source array cancelling the acoustic pressure and the *total* particle velocity component along the x-direction at the error sensor location (+) in a *uniform* primary sound field, i.e., a plane wave propagating in the z-direction. The two monopoles are located at $(\pm d/2, 0)$ and the error sensor is located at $(x, y) = (L, 0)$. The mean square pressure plots show the primary acoustic field (dashed line), the secondary acoustic field (dash-dot line) and the total acoustic field (dotted line) after control. Right column: equivalent graphs if a single monopole secondary source at $(x, y) = (0, 0)$ is used to cancel the pressure only at the same error sensor position. The plots correspond to $kL = 0{\cdot}5$ and the continuous and dotted lines represent reductions in the primary field of 10 and 20 dB, respectively.

zone of quiet in the x-direction is mainly caused by the reduction of the spatial rate of change of the secondary field at the cancellation point.

Figures 3 and 4 show the calculated average zones of quiet in a diffuse primary field for different frequencies using the strategies of pressure cancellation with one monopole secondary source and pressure and total particle velocity component cancellation at the same field point with a two-monopole secondary source array, respectively. For each frequency or value of kL, the average diffuse field zones of quiet have been calculated by averaging the squared modulus of the controlled fields from 20 samples of diffuse primary field and dividing the result by the average of the squared modulus of all the primary fields [5]. It can be seen that, up to about $kL = 1$, the extent of the zones along the radial and tangential directions after cancellation of the pressure and the total particle velocity

component increases considerably with respect to the case of cancelling the acoustic pressure only. Since the zones of quiet in Figure 4 have been calculated in the near field of a two-monopole array, the spatial arrangement of these two monopoles must have an effect on the geometry of the zones of quiet. The effect of the distance between the two secondary monopoles, d, compared with the distance of the mid-point to the microphone, L, on the diffuse field zones of quiet has been investigated. A set of simulations for the same kL values as the ones to be shown later in Figure 6 has been carried out but upon the assumption that ratio $d/L = 0{\cdot}25$. Comparing the results of these simulations with the contour plots in Figure 4 shows that the overall extension and shape of the diffuse field zones of quiet are not very sensitive to the distance between the two monopoles. As will be shown later, when the two monopoles are very close together the values of their respective source strengths increase significantly to the extent that the practical

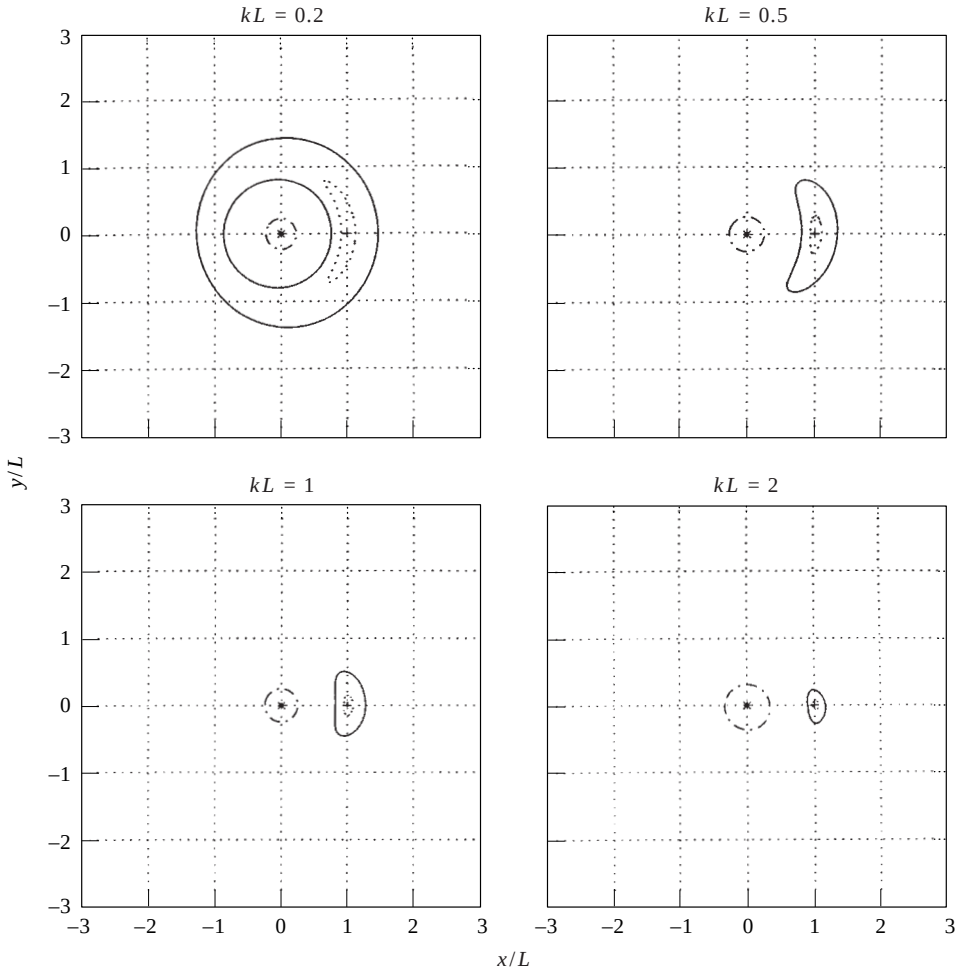

Figure 3. The average diffuse field zones of quiet for different values of kL, created by a single-monopole secondary source located at $(x, y) = (0, 0)$ cancelling the acoustic pressure at $(x, y) = (L, 0)$. The continuous and dotted lines correspond to reductions in the primary field of 10 and 20 dB, respectively. The dash-dot line corresponds to an increase in the primary field of 10 dB.

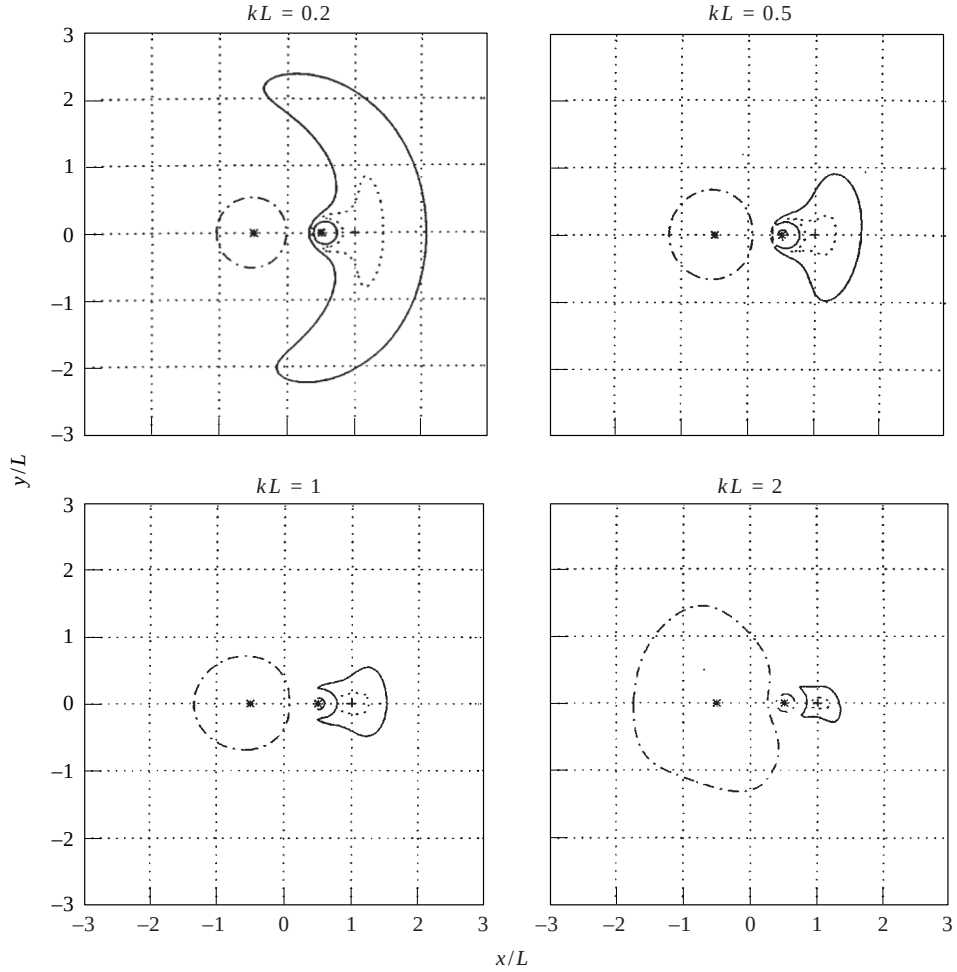

Figure 4. The average diffuse field zones of quiet for different values of kL, created by a two-monopole secondary source array with mid-point located at $(x, y) = (0, 0)$, cancelling the acoustic pressure and the *total* particle velocity component in the x-direction at $(x, y) = (L, 0)$. In these plots $d/L = 1$, where d is the distance between the monopoles. The continuous and dotted lines correspond to reductions in the primary field of 10 and 20 dB, respectively. The dash-dot line corresponds to an increase in the primary field of 10 dB.

realisation of such a system might become unrealistic. This is due to the fact that when d is small the pressure fields due to the two monopoles interact very strongly making the overall radiation efficiency of the array very low.

The secondary source model used so far is an array of monopoles which do not produce diffraction effects on the secondary and primary sound field. In a realistic local active noise control system, the secondary source will have a finite dimension and the diffraction effects caused by the secondary source cabinet on the secondary sound field are particularly important to understand the generated near field zone of quiet [6]. Previous work has shown that loudspeaker secondary source of the type used in a local active noise control system can be satisfactorily modelled in the frequency range of interest as a spherical source with an active segment [6].

This simple model can thus be used to predict the increase in the extent of the zone of quiet that can be achieved if the simultaneous control of pressure and particle velocity is implemented in a local active noise control system.

Figure 5 shows the extent of the zone of quiet produced by a spherical source of radius 0·08 m with an active segment of 50° and a ring, of maximum angle 120°, cancelling the pressure and the total particle velocity component in the x-direction at a point located at $(x, y) = (0{\cdot}19, 0)$ m. The primary sound field has been assumed diffuse and the computations have been carried out for $f = 109$, 273, 546 and 1092 Hz. These frequency values have been considered in order to be consistent with previous work [5, 6]. In these contour plots the frequency instead

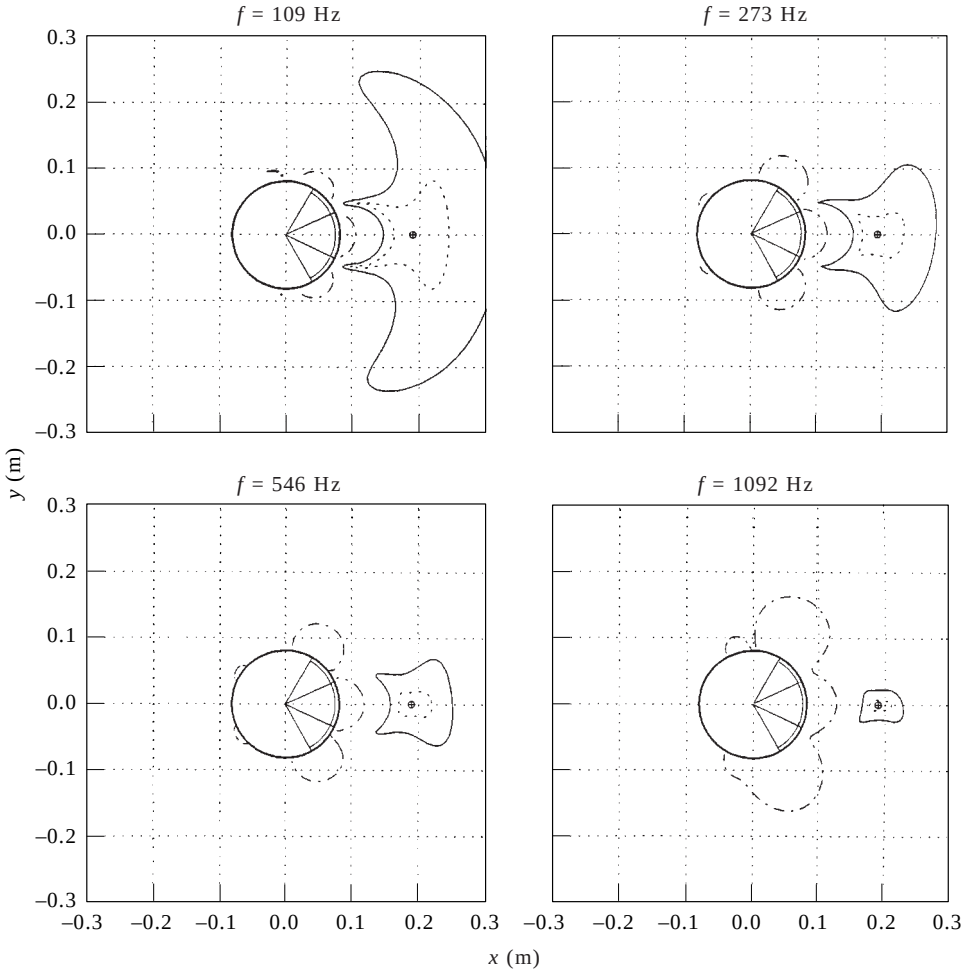

Figure 5. The calculated average acoustic field in the x–y plane due to the superposition of a diffuse primary acoustic field and the sound field due to a secondary spherical source of radius 0·08 m with an active segment of 50° and a ring of maximum angle 120° cancelling the acoustic pressure and the *total* particle velocity component in the x-direction at an error sensor located at $(x, y) = (0{\cdot}19, 0)$ m. The plots correspond to frequencies of 109, 273, 546 and 1092 Hz. The continuous and dotted lines correspond to reductions in the primary field of 10 and 20 dB, respectively. The dash-dot line corresponds to an increase in the primary field of 10 dB.

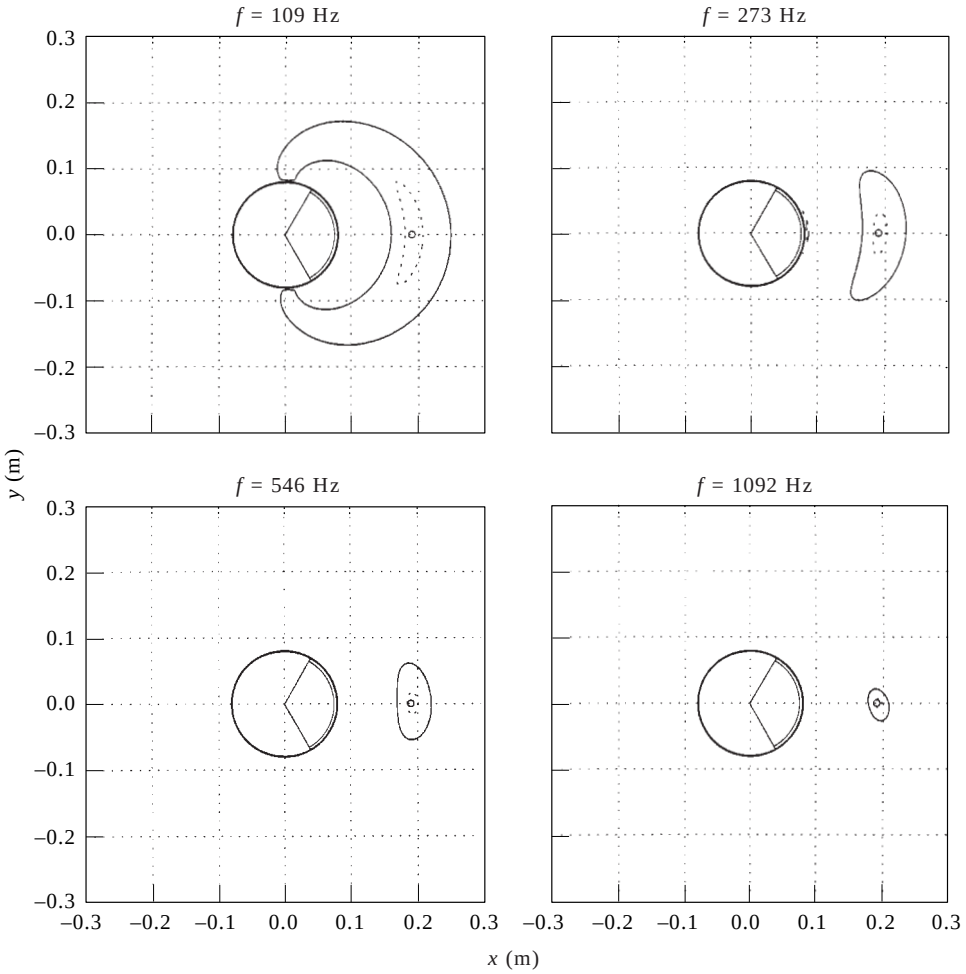

Figure 6. The calculated average acoustic field in the x–y plane due to the superposition of a diffuse primary acoustic field and the sound field due to a secondary spherical source of radius 0·08 m with an active segment of 120° cancelling the pressure at an error sensor located at $(x, y) = (0{\cdot}19, 0)$ m. The plots correspond to frequencies of 109, 273, 546 and 1092 Hz. The continuous and dotted lines correspond to reductions in the primary field of 10 and 20 dB, respectively.

of the kL value is used because for a finite sized secondary source, like the sphere with an active segment in this case, the distance L is not defined. These results should be compared with those depicted in Figure 6 which correspond to the average diffuse field zones of quiet produced by a spherical source with an active segment of angle 120° cancelling the acoustic pressure only at the same point as in Figure 5. The primary sound field in Figures 5 and 6 has been assumed diffuse and the results depicted represent the average zones in quiet based on an ensemble of 20 samples of diffuse fields each of which was generated by adding the contribution from 72-plane waves with random phase and equal amplitude arriving from uniformly distributed directions in the space [5, 6]. One can observe that the simultaneous cancellation of pressure and total particle velocity

component produces a considerable increase in the extent of the near field zones of quiet up to a frequency of about 500 Hz in this case. This increase is particularly important at low frequencies. However, as the frequency increases the cancellation of pressure and total particle velocity component does not produce any increase in the extent of the zone of quiet with respect to the case of cancelling the acoustic pressure only. Previous work [7] has shown that a practical local active noise control system in a headrest may be useful up to a frequency of approximately 500 Hz. This suggests that the cancellation of the acoustic pressure and the total particle velocity component can be of practical interest in the implementation of a local active noise control system.

4. ACTIVE CANCELLATION OF ACOUSTIC PRESSURE AND PARTICLE VELOCITY COMPONENT DUE TO THE SECONDARY SOURCE

If the point where the total particle velocity is cancelled is located in the near field of the secondary source, the total particle velocity is due mainly to the secondary field contribution. This is due to the fact that in the near field of a secondary source the spatial pressure gradient of the primary field is small compared with that of the secondary field. In order to illustrate this fact, the three types of secondary sources shown in Figure 7 are considered: i.e., a monopole, a spherical source with an active segment and a piston in a baffle. Since the particle velocity associated with a propagating wave is proportional to the spatial gradient of the acoustic pressure, a parameter that can be used to describe the spatial rate of change of a secondary acoustic field with respect to the associated acoustic pressure at the same point is the specific acoustic admittance (or inverse of the specific acoustic impedance), defined as

$$m_{sr} = u_{sr}/p_s, \tag{5}$$

where u_{sr} and p_s denote the acoustic particle velocity component in the r direction and the acoustic pressure associated with the secondary sound field, respectively.

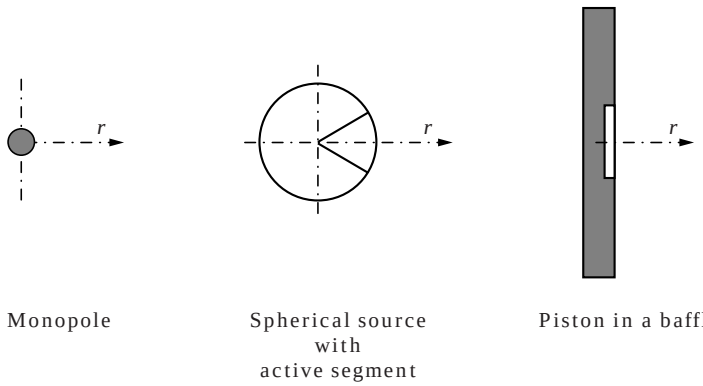

Figure 7. The three types of secondary acoustic sources used to study the spatial change of the acoustic pressure at a point in the near field of a source with respect to the value of the pressure at the same point.

In many practical applications of a local active noise control system, the primary pressure field will be due to a large number of acoustic modes excited in an enclosure. Therefore, a suitable assumption to estimate the average performance of such a local active noise control system is to consider the primary sound field as diffuse. It is known that in a diffuse sound field the space-average mean square particle velocity component in an arbitrary direction, $\langle|u_d|^2\rangle$ is equal to [8]

$$\langle|u_{dr}|^2\rangle = \langle|p_d|^2\rangle/3(\rho_o c_o)^2, \tag{6}$$

where $\langle|p_d|^2\rangle$ is the space average mean square pressure of the diffuse field, $\langle|u_{dr}|^2\rangle$ is the space average mean square particle velocity component, ρ_o is the density of air and c_o is the speed of sound. From equation (6) one can define the space-average mean square acoustic admittance of the diffuse field as

$$\langle|m_{dr}|^2\rangle = \langle|u_{dr}|^2\rangle/\langle|p_d|^2\rangle = 1/3(\rho_o c_o)^2. \tag{7}$$

Squaring equation (5) and dividing it by equation (7) yields a non-dimensional parameter that describes the relative spatial gradient per unit pressure of the secondary field with respect to that associated with a primary diffuse sound field: i.e.,

$$\frac{|m_{sr}|^2}{\langle|m_{dr}|^2\rangle} = \frac{|u_{sr}|^2/|p_s|^2}{\langle|u_{dr}|^2\rangle/\langle|p_d|^2\rangle}. \tag{8}$$

For a monopole source, equation (8) gives

$$\left.\frac{|m_{sr}|^2}{\langle|m_{dr}|^2\rangle}\right|_{monopole} = 3\left(\frac{1}{(kr)^2} + 1\right), \tag{9}$$

where k is the wavenumber and r denotes the distance between the monopole and the field point (see Figure 7). For a piston of radius a in an infinite baffle [9], equation (8) gives, after some algebra,

$$\left.\frac{|m_{sr}|^2}{\langle|m_{dr}|^2\rangle}\right|_{piston} = \frac{3}{4}\frac{1 + \dfrac{1}{1+(a/r)^2} - \dfrac{2}{\sqrt{1+(a/r)^2}}\cos\left(kr(1-\sqrt{1+(a/r)^2})\right)}{\sin^2\left(\dfrac{kr}{2}(1-\sqrt{1+(a/r)^2})\right)}. \tag{10}$$

For the case of a spherical source with an active segment, expression (8) can be calculated by expanding the secondary acoustic pressure at a point (r, θ) outside the spherical source with a sinusoidally pulsating segment aligned along the azimuthal co-ordinate as [10]

$$p(r, \theta) = \sum_{m=0}^{\infty} A_m \mathrm{P}_m(\cos\theta)\mathrm{h}_m^{(2)}(kr), \tag{11}$$

where $P_m(\cos\theta)$ is the Legendre polynomial of order m and $\mathrm{h}_m^{(2)}(kr)$ is the spherical Hankel function of the second kind of order m. A_m denotes the pressure coefficient associated to the mth spherical harmonic and have to be determined to calculate

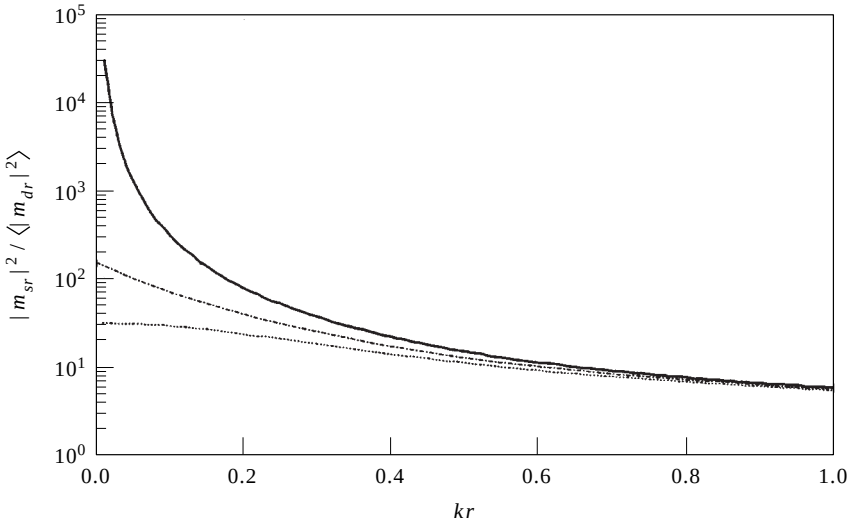

Figure 8. The ratio of the square of the modulus of the specific acoustic admittance associated with the secondary sound field produced by the acoustic sources of Figure 7 with respect to the space-average mean square specific acoustic admittance of a diffuse field. The continuous line has been calculated with equation (9) (monopole), the dash-dot line with equation (12) (spherical source of radius 0·05 m and segment of 90°) and the dotted line corresponds to equation (10) (piston with radius 0·05 m).

the value of $p(r, \theta)$. From equation (11) the radial surface velocity can be calculated on the surface of the spherical source. By matching this radial velocity with that of the radiator the pressure coefficients A_m can be determined. Morse [11] has solved this problem analytically but here a numerical method has been used which has also been applied to the two-sphere problem used for the simulations presented later. After some algebra, it can be shown that the value of expression (8) for points on-axis of the spherical source with an active segment of Figure 7 can be expressed as

$$\left.\frac{|m_{sr}|^2}{\langle |m_d|^2 \rangle}\right|_{segment} = 3 \frac{\left(\sum_{m=0}^{\infty} A_m \mathrm{P}_m(1) \mathrm{h}_m^{(2)}(kr) \right)^2}{\left(\sum_{m=0}^{\infty} A_m \mathrm{P}_m(1) \mathrm{h}_m^{(2)}(kr) \right)^2}, \tag{12}$$

where $\mathrm{h}_m^{(2)}$ denotes the derivative of the spherical Hankel function of the second kind of order m with respect to the spatial variable r. Figure 8 shows the value of the expression (8) for the three sources in Figure 7 as a function of kr. The radius of the spherical source has been assumed equal to 0·05 m with an active segment of 90° and the radius of the piston is 0·05 m. The curves for these two

types of sources have been calculated upon assuming $k = 2\pi$ and taking different values of r. It is clear from Figure 8 that for the majority of secondary sources and the range of kL values (where L is the distance between the centre of the source and the cancellation point) that can be used in a practical local active noise control system, i.e., $kL < 1$, the total particle velocity component in the axial direction of the source is mainly due to the contribution of the secondary field. This suggests that the zones of quiet produced after the cancellation of the acoustic pressure and the total particle velocity component in the near field of a secondary source must be similar to those generated when cancelling the pressure and the secondary particle velocity, i.e., the particle velocity due to the secondary source only.

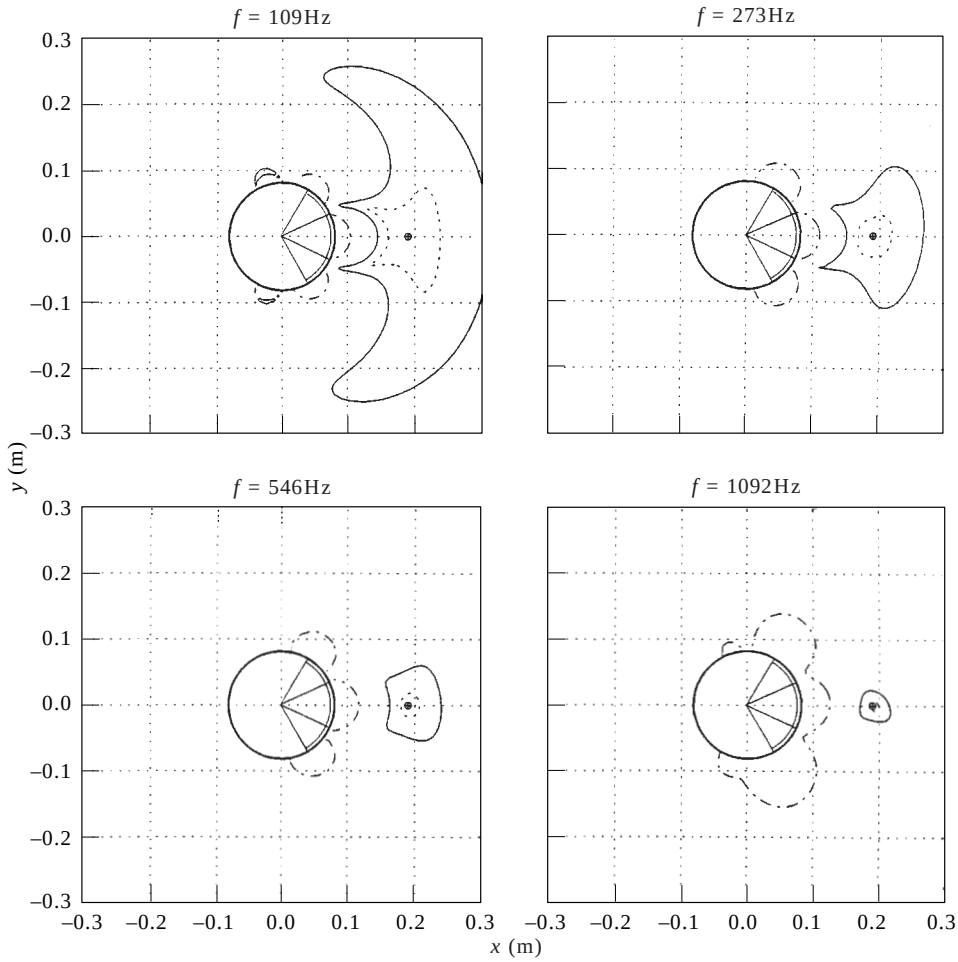

Figure 9. The calculated average acoustic field in the x–y plane due to the superposition of a diffuse primary acoustic field and the sound field due to a secondary spherical source of radius 0·08 m with an active segment of 50° and a ring of maximum angle 120° cancelling the pressure and the *secondary* particle velocity component in the x-direction at an error sensor located at $(x, y) = (0{\cdot}19, 0)$ m. The plots correspond to frequencies of 109, 273, 546 and 1092 Hz. The continuous and dotted lines correspond to reductions in the primary field of 10 and 20 dB, respectively. The dash-dot line corresponds to an increase in the primary field of 10 dB.

5. NEAR FIELD ZONES OF QUIET AFTER CANCELLATION OF TOTAL ACOUSTIC PRESSURE AND PARTICLE VELOCITY COMPONENT DUE TO THE SECONDARY SOURCE

Figure 9 shows the diffuse field zones of quiet generated by a spherical source with an active segment and a ring cancelling the pressure and the secondary particle velocity component along the x-direction. The geometry of this source corresponds to that in Figure 5. As expected, the average zones of quiet obtained when using this strategy are very similar to those obtained when cancelling the pressure and the total particle velocity component in the same direction (see Figure 5). These simulations suggest that a local active noise control system cancelling the acoustic pressure and the secondary particle velocity will perform acoustically in a way similar to that of a system that cancels the pressure and the total particle velocity. The main advantage of cancelling the secondary particle velocity instead of the total particle velocity component is that a velocity sensor is no longer necessary. All that is needed is the knowledge of the transfer functions that relate the strength of each active surface of the secondary source array with their respective particle velocity component in a given direction at the cancellation point. This information allows us to calculate the amplitude and phase relationship between the two active surfaces to achieve the cancellation of the secondary particle velocity at the selected field point.

Since a practical local active noise control system generally has to be implemented close to a listener's head, the effect of such a diffracting body on both the secondary and the primary sound field must have an effect on the generated zones of quiet. It is known that the diffraction produced by a listener's head on the zones of quiet generated by a practical local active noise control system can be suitably modelled as a spherical source with an active segment radiating close to a rigid sphere [6, 7]. The same approach is considered here to estimate the effect that a diffracting head has on the zones of quiet produced when the acoustic pressure and the secondary particle velocity component are cancelled in the near field of a secondary source. Figure 10 shows the average diffuse field zone of quiet produced by a spherical source with an active segment and a ring, as in Figure 9, when both the acoustic pressure and the secondary particle velocity are cancelled at a point near a rigid sphere. As expected, the presence of the rigid sphere does not deteriorate the extent of the zone of quiet and, if the rigid sphere is close enough to the cancellation point, the zone of quiet is attached to the sphere [6]. The results depicted in Figure 10 can be compared with those in Figure 11 which shows the average diffuse field zone of quiet produced by a spherical source with an active segment of 120° cancelling the acoustic pressure only at the same position near the rigid sphere for the same frequency values. Similar results have been presented in reference [6] but these are reproduced here for completeness. By comparing the results shown in Figures 10 and 11 it can be concluded that the simultaneous cancellation of the acoustic pressure and the secondary acoustic particle velocity component in the x-direction near a diffracting head produces a desirable increase in the extent of the zone of quiet along the direction of the cancelled velocity component and also in the perpendicular direction. These results suggest that this strategy may be useful in a practical local active noise control

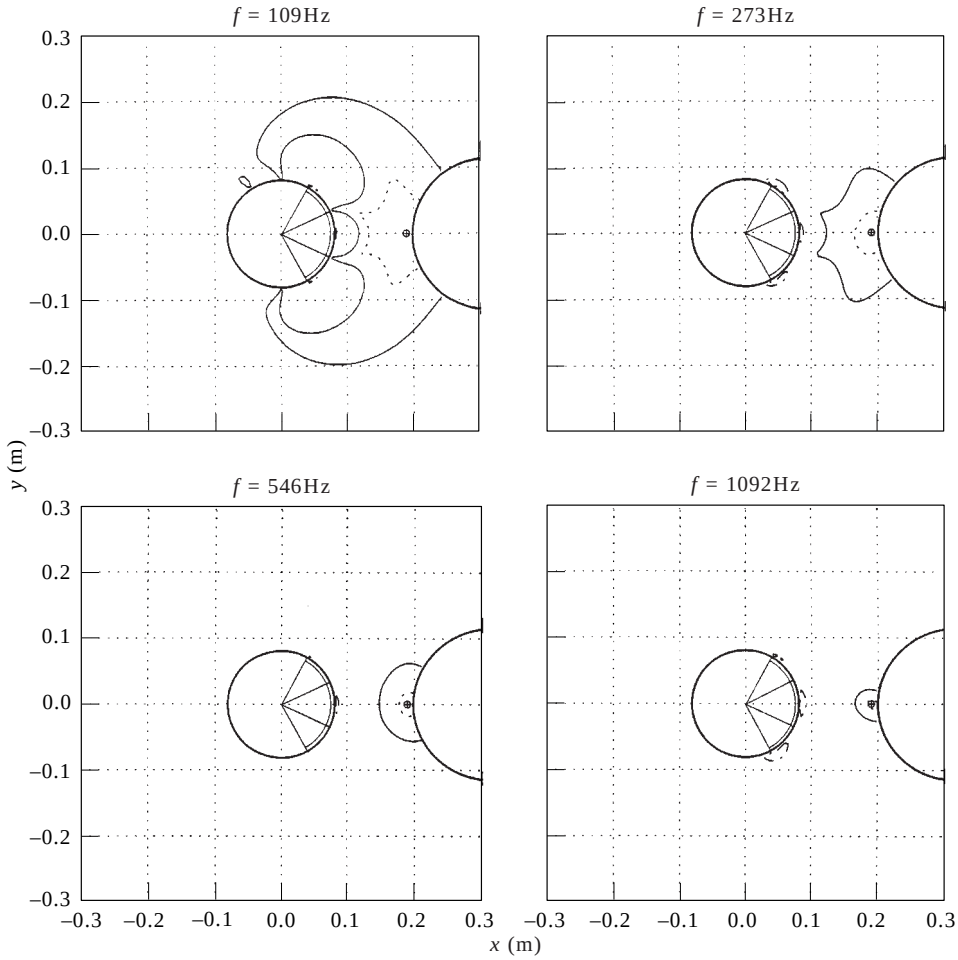

Figure 10. The calculated average acoustic field in the x–y plane due to the superposition of a diffuse primary acoustic field and the sound field due to a secondary spherical source of radius 0·08 m with an active segment of 50° and a ring with a maximum angle of 120°, cancelling the pressure and the *secondary* particle velocity component in the x-direction at a point located at $(x, y) = (0{\cdot}19, 0)$ m close to a rigid sphere. The radius of the rigid sphere is 0·115 m and its centre is located at 0·315 m from the centre of the spherical source. The plots correspond to frequencies of 109, 273, 546 and 1092 Hz. The continuous and dotted lines correspond to reductions in the primary field of 10 and 20 dB, respectively. The dash-dot line corresponds to an increase in the primary field of 10 dB.

system working near a listener's head where the fact that the secondary pressure gradients are very high near the secondary source is one of the factors that limits the extent of the zones of quiet.

6. PRACTICAL LIMITATIONS FOR ACOUSTIC VELOCITY COMPONENT CANCELLATION

For the particular case of the two-monopole secondary source array of Figure 1, the cancellation of the secondary particle component in the x-direction at a field point $(L, 0)$ requires that

$$q_{s1} T_{u_x s1}(L, 0) + q_{s2} T_{u_x s2}(L, 0) = 0, \tag{13}$$

were q_{s1} and q_{s2} have been defined in equation (1), and $T_{u_x s1}(r, \theta)$ and $T_{u_x s2}(r, \theta)$ can be expressed, after equation (2b) as

$$T_{u_x s1}(L, 0) = \frac{e^{-jkr_1}}{4\pi} \cdot \left(\frac{jk}{r_1} + \frac{1}{r_1^2}\right), \qquad T_{u_x s2}(L, 0) = \frac{e^{-jkr_2}}{4\pi} \cdot \left(\frac{jk}{r_2} + \frac{1}{r_2^2}\right), \tag{14}$$

where $r_1 = L - d/2$ and $r_2 = L + d/2$. By substituting the expressions (14) into equation (13), it can be shown that the cancellation of the secondary particle

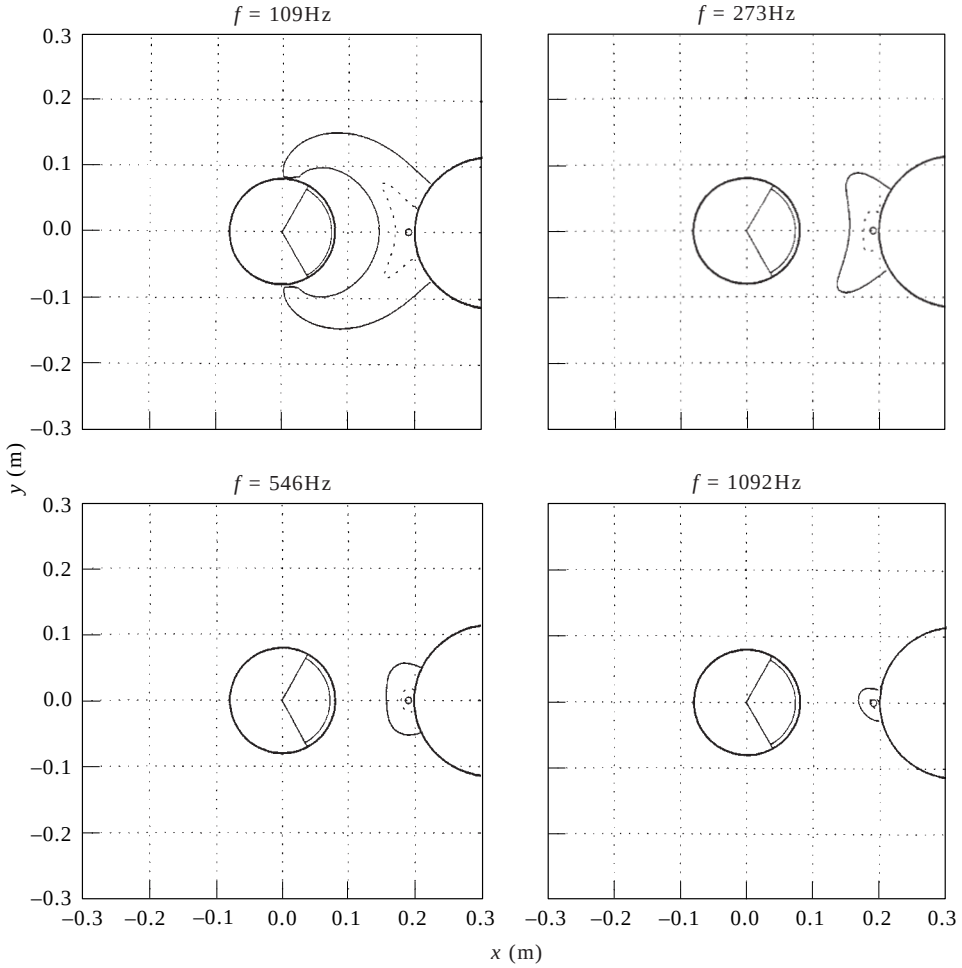

Figure 11. The calculated average acoustic field in the x–y plane due to the superposition of a diffuse primary acoustic field and the sound field due to a secondary spherical source of radius 0·08 m with an active segment of 50°, cancelling the pressure only at a point located at $(x, y) = (0{\cdot}19, 0)$ m close to a rigid sphere. The radius of the rigid sphere is 0·115 m and its centre is located at 0·315 m from the centre of the spherical source. The plots correspond to frequencies of 109, 273, 546 and 1092 Hz. The continuous and dotted lines correspond to reductions in the primary field of 10 and 20 dB, respectively.

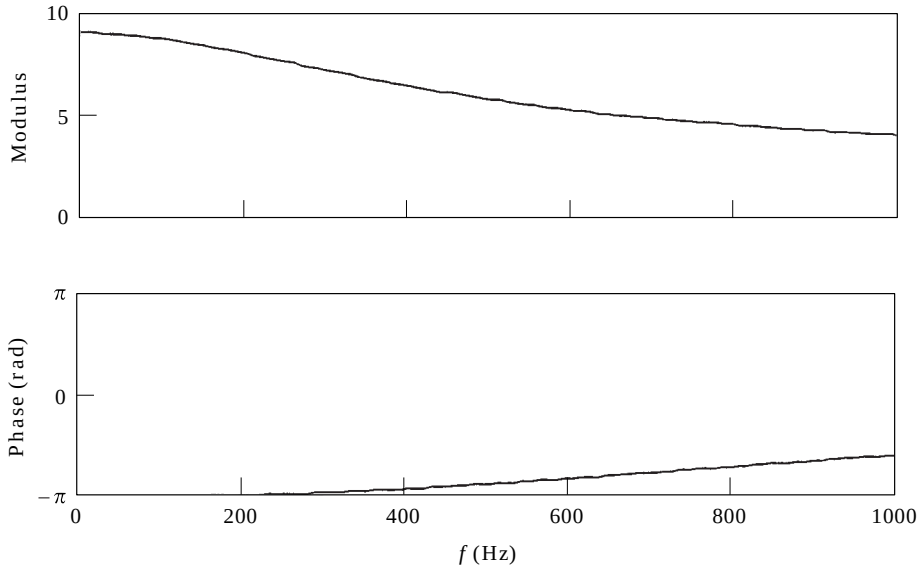

Figure 12. Ratio q_{s2}/q_{s1} for two monopoles a distance $d = 0{\cdot}1$ m apart creating a total secondary field whose on-axis particle velocity component at $(x, y) = (L, 0)$, with $L = 0{\cdot}1$ m, is zero.

velocity component in the x-direction at $(L, 0)$ requires that the ratio of the two-monopole sources satisfies the expression

$$\frac{q_{s2}}{q_{s1}} = -\left(\frac{L + d/2}{L - d/2}\right)^2 \mathrm{e}^{\mathrm{j}kd} \cdot \frac{1 + \mathrm{j}k(L - d/2)}{1 + \mathrm{j}k(L + d/2)}. \tag{15}$$

The modulus and phase of this complex ratio for the particular case of $L = d = 0{\cdot}1$ m is illustrated in Figure 12. It is interesting to observe that at low frequencies $q_{s2} \cong -9q_{s1}$, and that this simple relationship is valid for a relatively large frequency range. This suggests that in order to cancel the particle velocity at one point in the near field of a secondary source array, the source furthest from the cancellation point must be driven much harder than the other, perhaps making the control system impractical. In the low frequency limit the ratio q_{s2}/q_{s1} in equation (15) converges to

$$\frac{q_{s2}}{q_{s1}} = -\left(\frac{L + d/2}{L - d/2}\right)^2 = -\left(\frac{L/d + 1/2}{L/d - 1/2}\right)^2 \quad \text{for } kL \ll 1, \tag{16}$$

which is equal to -9 for the case shown in Figure 12. Figure 13 depicts equation (16) as a function of L/d, which indicates that as L/d approaches $1/2$, the ratio q_{s2}/q_{s1} tends to infinity. This particular condition corresponds to the case when the cancellation point is located at the same position as q_{s1}. Figure 13 also suggests that in order to avoid high values of the ratio q_{s2}/q_{s1} in a practical local active noise control system seeking to cancel the acoustic pressure and the secondary particle velocity component at a position $(L, 0)$, the distance from the mid-point of the

source array to the microphone, L, should be greater than the monopole source separation in the secondary source array, d: i.e., $L/d > 1$.

If the two monopole sources are adjusted so that equation (15) is satisfied, the total secondary acoustic pressure produced by the monopole source array can be expressed as

$$p_s = \frac{j\omega\rho_o}{4\pi} q_{s1}\left[\frac{e^{-jkr_1}}{r_1} - \left(\frac{L + d/2}{L - d/2}\right)^2 e^{jkd}\frac{1 + jk(L - d/2)}{1 + jk(L + d/2)}\frac{e^{-jkr_2}}{r_2}\right], \tag{17}$$

where r_1 and r_2 have been defined in equation (2b).

A way of estimating the additional "cost" associated with the cancellation of the particle velocity is to calculate the ratio between the sum of the squared volume velocities required to cancel pressure and secondary particle velocity and that required to cancel the pressure only: i.e.,

$$\frac{|q_{s1}|^2 + |q_{s2}|^2}{|q_{s-mono}|^2}, \tag{18}$$

where $q_{s\text{-}mono}$ is the source strength of a single monopole located at $(-d/2, 0)$ cancelling the pressure at $(L, 0)$. Figure 14 shows the value of equation (18) calculated up to $kL = 2$ for different values of the ratio L/d and upon assuming $L = 0{\cdot}1$ m. It is clear from these results that a practical local control system using two secondary sources to cancel the acoustic pressure and the secondary particle velocity at a point in its near field with, say, $0{\cdot}1 \text{ m} < L < 0{\cdot}15$ m, has to keep the two active surfaces a distance apart such that $d \geqslant L$, but even then the ratio given by equation (18) takes a value of about 5 at $kL = 2$. The results shown in Figure 14 suggest that in a practical local active noise control the point of secondary velocity component cancellation should be as close as possible to the secondary

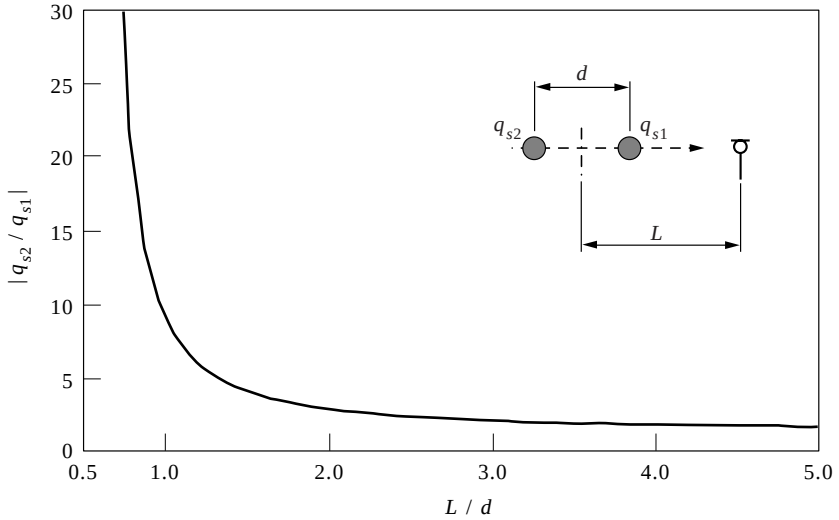

Figure 13. Low frequency limit for the ratio q_{s2}/q_{s1} for two monopoles a distance d apart creating a total secondary field whose on-axis particle velocity component at $(x, y) = (L, 0)$ is zero. The curve has been calculated with equation (16).

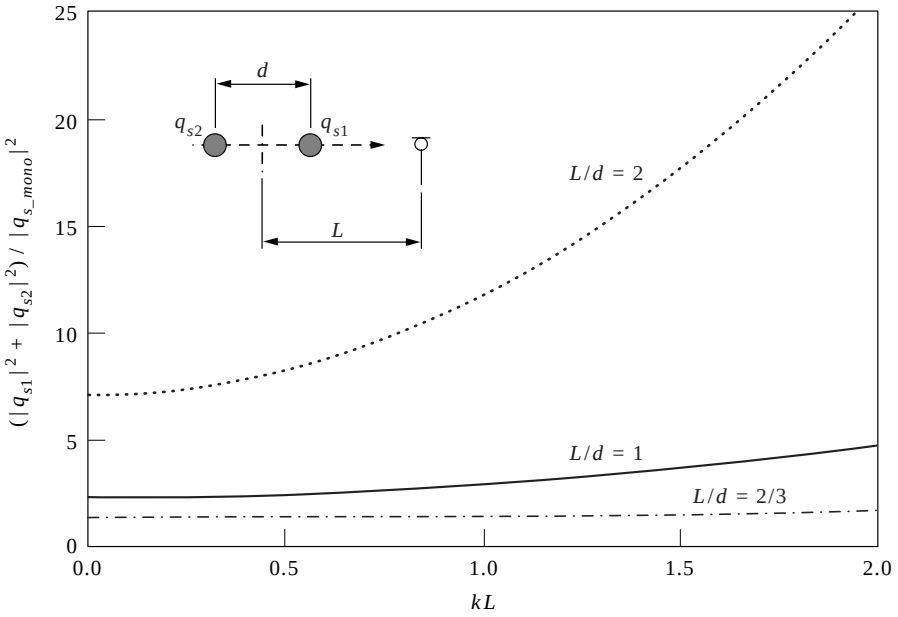

Figure 14. Ratio of the sum of the squared modulus of the two monopole secondary sources, at a distance d apart, satisfying equation (15) and cancelling the pressure and secondary particle velocity component along the x-axis at a point $(L, 0)$, to the squared modulus of the monopole source strength at $(-d/2, 0)$ cancelling the pressure at the same cancellation point (see equation (18)). The results have been calculated for $L = 0{\cdot}1$ m.

source array. However, in order to obtain high attenuation at the ear positions, the point of pressure cancellation has to be as close as possible to the listener's ears. This suggests that the cancellation of the pressure and the secondary particle velocity at two different points in the near field of a secondary source array may be of practical interest. Figures 15 and 16 show the average diffuse field zones of quiet generated by a spherical source with an active segment and a ring cancelling the acoustic pressure and the secondary particle velocity at two different points with a diffracting sphere present. The point of pressure cancellation is denoted with a small circle ($\bigcirc$) and the location of the secondary particle velocity cancellation with a cross ($+$). The distances between the point of velocity cancellation and the surface of the spherical source in Figures 15 and 16 are 0·07 and 0·02 m, respectively, and the point of pressure cancellation is located at 0·01 m from the surface of the diffracting head. These results suggest that cancelling the secondary acoustic velocity at a field point located between the point of pressure cancellation and the secondary source produces zones of quiet similar to those created when the pressure and the velocity component are cancelled at the same point close to the rigid sphere (see Figure 10). However, if the secondary velocity is cancelled at a point very close to the secondary source, the extent of the zones of quiet decreases and its shape becomes very similar to that obtained if only the acoustic pressure was cancelled (see Figure 11). It is interesting to note that the diffuse field zones of quiet shown in Figures 10 and 15 are fairly similar. In fact, locating the point of velocity cancellation closer to the secondary source seems to produce slightly larger zones of quiet along the x-direction than if the cancellation is carried

out at a point very close to the surface of the diffracting head. The results shown in Figures 10, 15 and 16 suggest that locating the point of secondary velocity cancellation at an intermediate position between the diffracting head and the secondary source may improve the extent of the zone of quiet along the line defined by the points of pressure and secondary particle velocity cancellation.

However, the cancellation of the acoustic pressure and the secondary particle velocity at different locations must have an effect on the relative effort required by the secondary source array. This relative effort can be estimated by using an expression similar to that defined in equation (18), which in the case of the

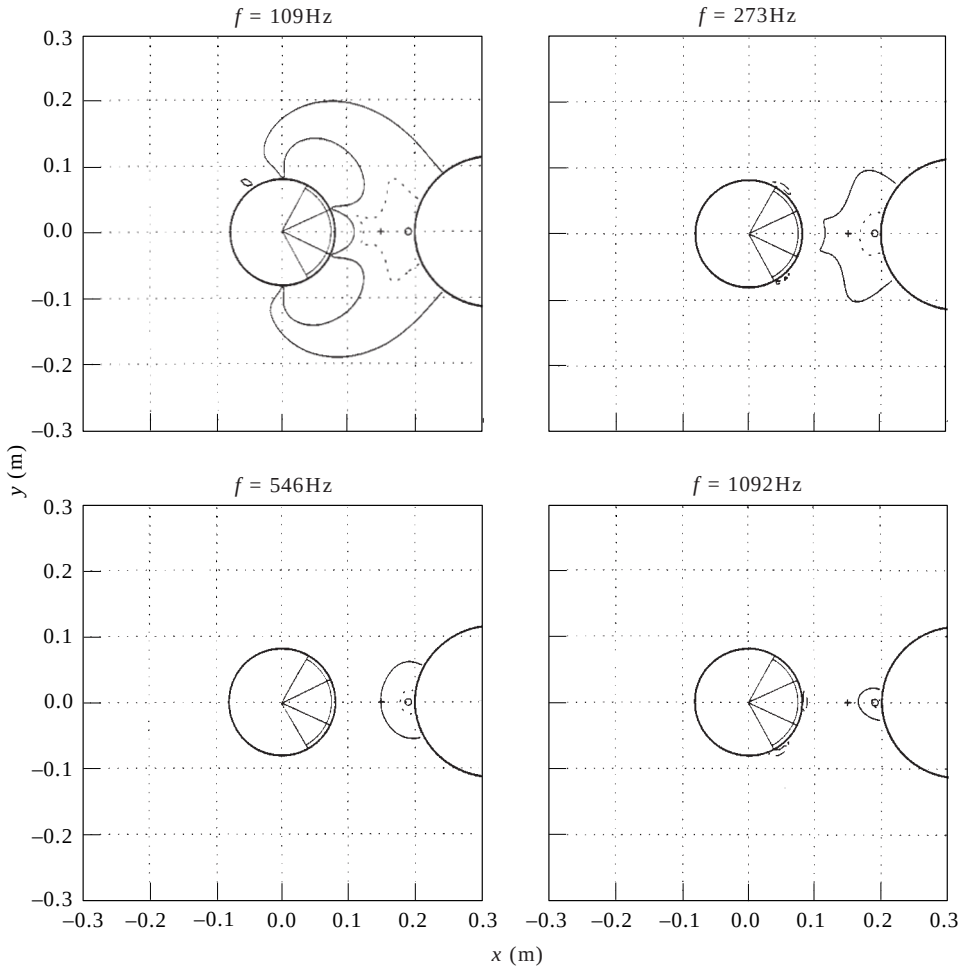

Figure 15. The calculated average acoustic field in the x–y plane due to the superposition of a diffuse primary acoustic field and the sound field due to a secondary spherical source of radius 0·08 m with an active segment of 50° and a ring with a maximum angle of 120°, cancelling the pressure at $(x, y) = (0{\cdot}19, 0)$ m close to a rigid sphere "○", and the *secondary* particle velocity component in the x-direction at a point located at $(x, y) = (0{\cdot}15, 0)$ m, "+". The radius of the rigid sphere is 0·115 m and its centre is located at 0·315 m from the centre of the spherical source. The plots correspond to frequencies of 109, 273, 546 and 1092 Hz. The continuous and dotted lines correspond to reductions in the primary field of 10 and 20 dB, respectively. The dash-dot line corresponds to an increase in the primary field of 10 dB.

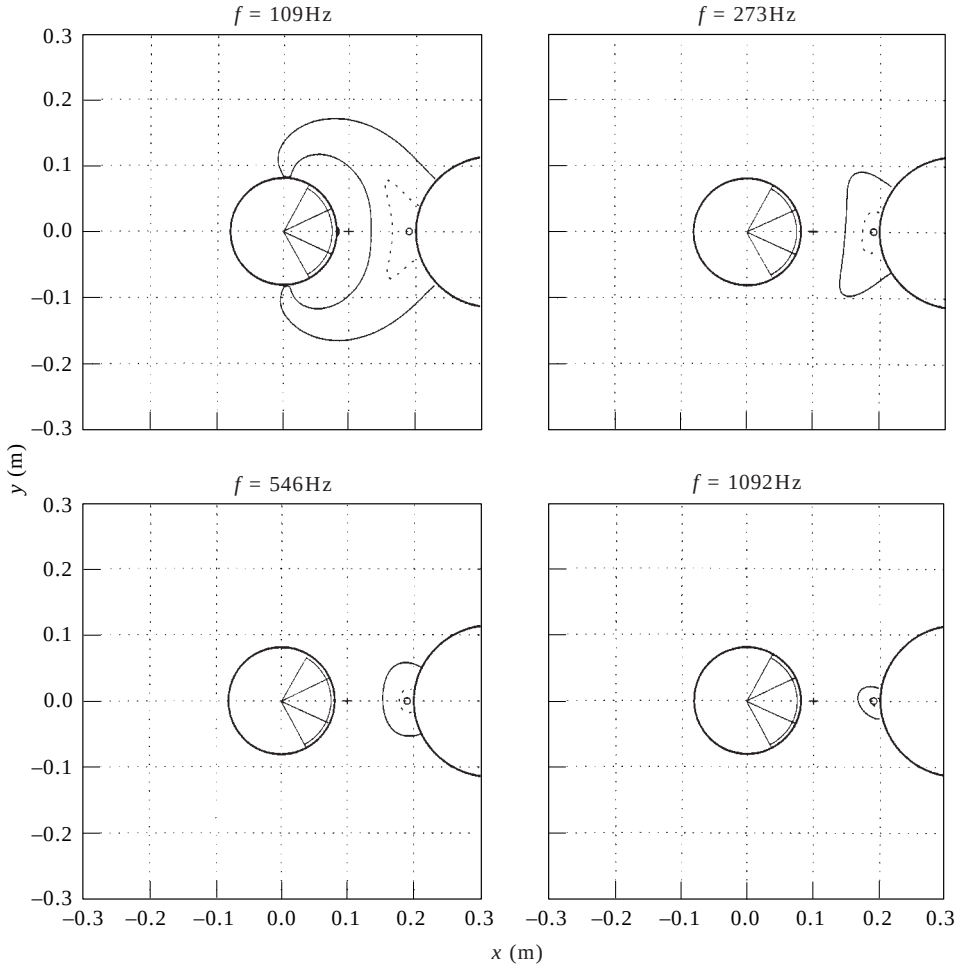

Figure 16. The calculated average acoustic field in the x–y plane due to the superposition of a diffuse primary acoustic field and the sound field due to a secondary spherical source of radius 0·08 m with an active segment of 50° and a ring with a maximum angle of 120°, cancelling the pressure at $(x, y) = (0{\cdot}19, 0)$ m close to a rigid sphere, "○", and the *secondary* particle velocity component in the x-direction at a point located at $(x, y) = (0{\cdot}10, 0)$ m, "+". The radius of the rigid sphere is 0·115 m and its centre is located at 0·315 m from the centre of the spherical source. The plots correspond to frequencies of 109, 273, 546 and 1092 Hz. The continuous and dotted lines correspond to reductions in the primary field of 10 and 20 dB, respectively.

spherical source with an active segment and a ring considered here would take the form

$$\frac{|q_{seg}|^2 + |q_{ring}|^2}{|q_{seg\ ref}|^2}, \tag{19}$$

where q_{seg} and q_{ring} are the volume velocities associated with the active segment and ring respectively in the spherical source considered above when the acoustic pressure and secondary particle velocity in the x-direction are cancelled, and $q_{seg\ ref}$ is the source strength of a reference segment whose angle is equal to the maximum angle of the active ring (120° in the case studied here), which is adjusted to cancel

the pressure only. Figure 17(a) depicts the value of the expression (19) for a spherical source of radius 0·08 m ($ka \approx 0{\cdot}4$) with an active segment of 50° and an active ring with maximum angle of 120° seeking to cancel the pressure and the secondary velocity at two different points located on-axis at distances L_p and L_u from the surface of the source, respectively. In this simulation the primary sound field has been assumed uniform and there is not a diffracting sphere present. Figure 17(a) suggests that in order to avoid high values of the cost function (19), for a given on-axis point of pressure cancellation, the location of the point of secondary

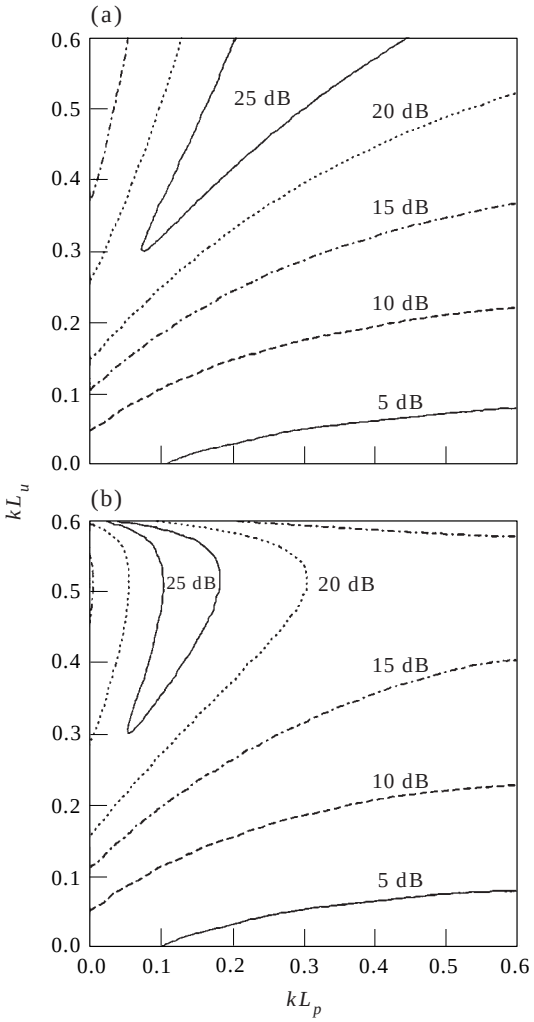

Figure 17. (a) The value of the expression (19) for a spherical source of $ka = 0{\cdot}4$ with an active segment of angle 50° and an active segment of 120° when the acoustic pressure and the secondary particle velocity component in the x-direction are cancelled at two different points located on-axis at distances L_p and L_u from the surface of the source respectively. q_{seg_ref} denotes the source strength of a reference segment of angle 120° cancelling only the pressure at the point located at a distance L_p from the source. The primary acoustic field has been assumed as uniform. (b) As (a), but with a rigid sphere of $ka = 0{\cdot}6$ present whose centre is 0·25 wavelengths from the centre of the spherical source.

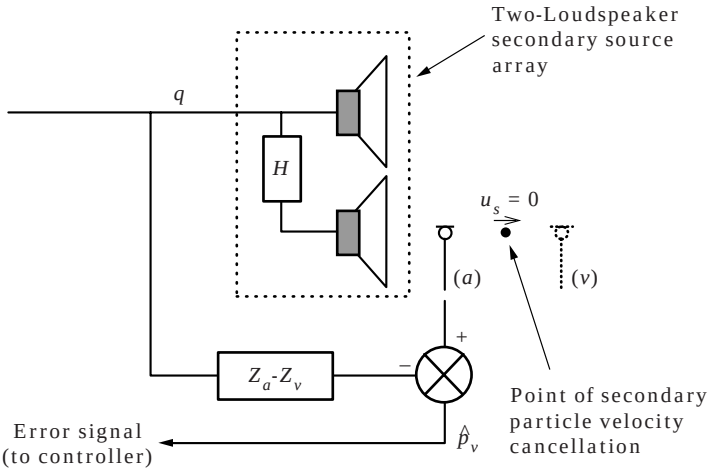

Figure 18. A single channel virtual microphone arrangement using a two-loudspeaker secondary source array to cancel the acoustic pressure at a virtual microphone position (v) and the secondary particle velocity component u_s at another point.

velocity component cancellation should be as close as possible to the source. Figure 17(b) shows the value of equation (19) when the spherical source is radiating near a diffracting sphere of radius 0·115 m ($ka' = 0{\cdot}6$, where a' is the radius of the rigid sphere) whose centre is at 0·315 m (0·25 wavelengths) from the centre of the spherical source. One can observe that the presence of a diffracting head reduces the value of the expression (19) when the point of secondary velocity cancellation is close to the rigid sphere, i.e., for high values of kL_u, with respect to the case when the rigid sphere is not present. This is due to the fact that if one tries to cancel the secondary velocity at a point very close to a rigid body and in the direction normal to the surface, the active parts of the secondary source array

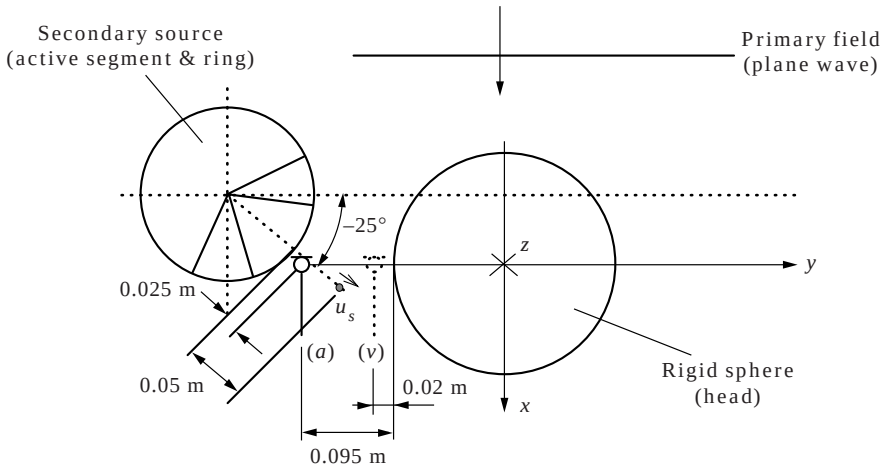

Figure 19. The two-sphere model used to predict the zone of quiet created when the two-loudspeaker source array of Figure 18 is adjusted to cancel the primary pressure at the virtual microphone position and the secondary particle velocity in the axial direction at a point position on the axis of the source and at a distance of 0·05 m from the source.

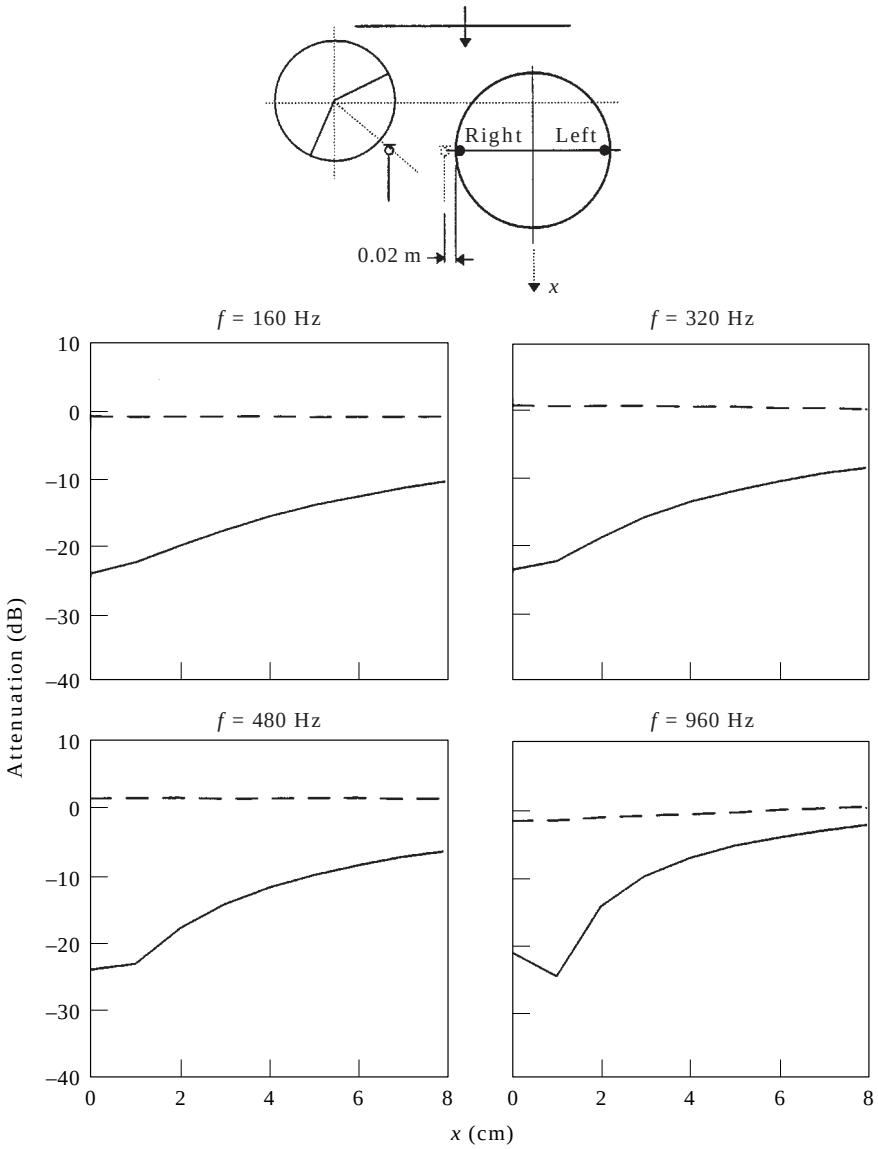

Figure 20. The calculated controlled acoustic field at the measuring points corresponding to the right (continuous) and left (dashed line) hand ears of the listener (black dots) when the secondary spherical source with an active segment seeks to cancel the primary acoustic field at a virtual microphone position, for different positions of the rigid sphere along the x-axis. The primary acoustic field is a plane wave propagating in the positive x-direction. $y = 0$, $z = 0$.

do not have to be driven very hard since the secondary velocities produced by each contributing vibrating surface are already close to zero. Figure 17 shows that in order to have low values for the expression (19), with or without a rigid sphere present, the position of the point of secondary velocity cancellation should be close to the source. However, Figures 15 and 16 show that if the secondary velocity is cancelled at a point too close to the secondary source, the extent of the zone of quiet decreases being similar to that obtained when only the acoustic pressure is

cancelled. This suggests that the definition of the field point of velocity cancellation in a practical local active control system involves a trade-off.

7. A PRACTICAL LOCAL ACTIVE NOISE CONTROL SYSTEM WITH A TWO-LOUDSPEAKER SOURCE ARRAY

It is known that the zone of quiet in the near field of a secondary source becomes larger as the error microphone is moved further away from the source [12]. To

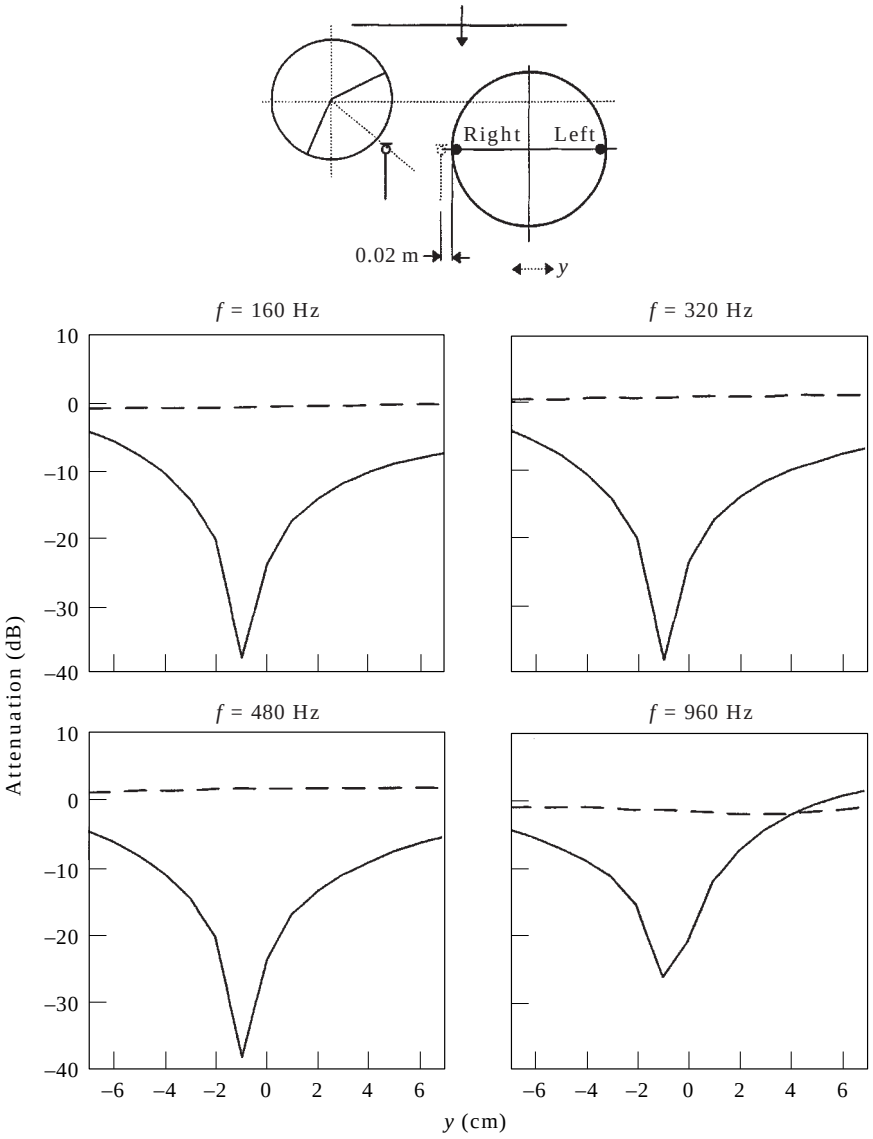

Figure 21. The calculated controlled acoustic field at the measuring points corresponding to the right (continuous) and left (dashed line) hand ears of the listener (black dots) when the secondary spherical source with an active segment seeks to cancel the primary acoustic field at a virtual microphone position, for different positions of the rigid sphere along the y-axis. The primary acoustic field is a plane propagating in the positive x-direction. $x = 0$, $z = 0$.

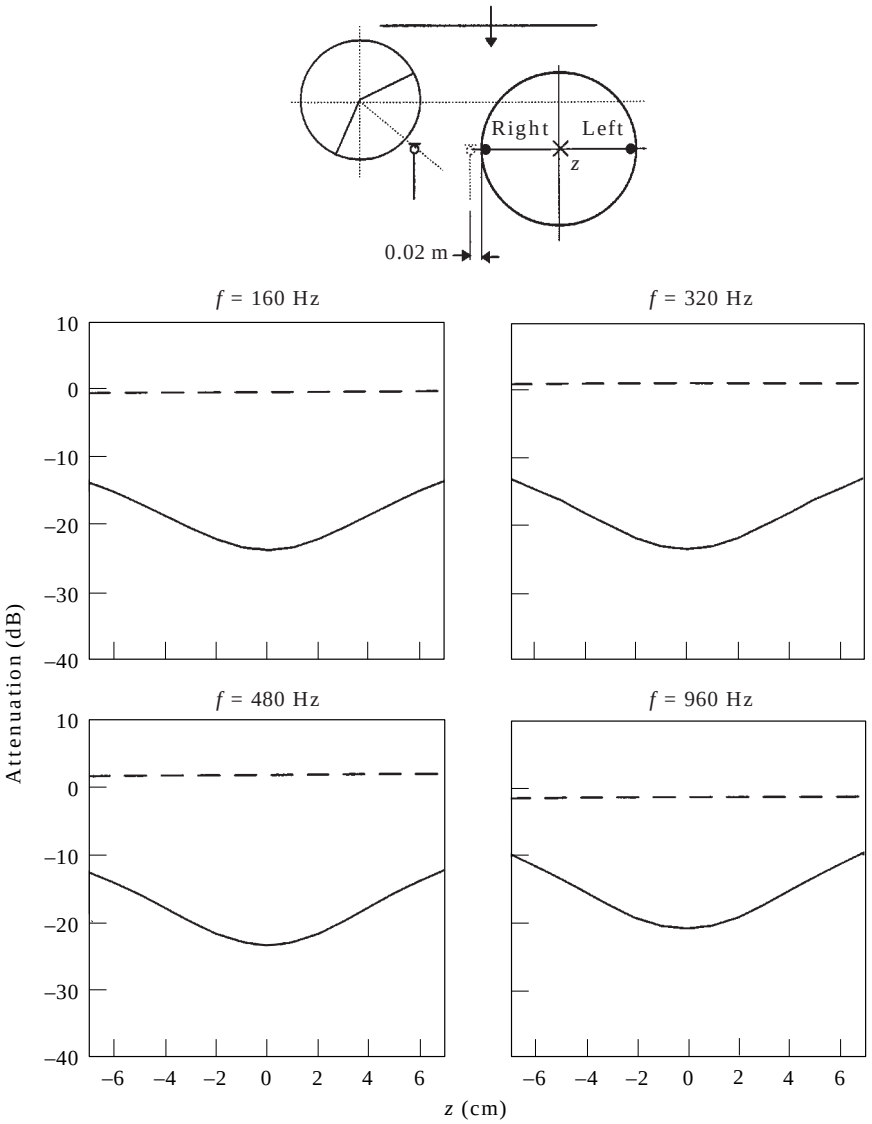

Figure 22. The calculated controlled acoustic field at the measuring points corresponding to the right (continous) and left (dashed line) hand ears of the listener (black dots) when the secondary spherical source with an active segment seeks to cancel the primary acoustic field at a virtual microphone position, for different positions of the rigid sphere along the z-axis. The primary acoustic field is a plane propagating in the positive x-direction. $x = 0$, $y = 0$.

produce useful-sized zones of quiet, the error microphone may thus have to be at an inconveniently large distance from the secondary source and may then interfere with the movement of the listener's head. Elliott and David [13] have proposed an arrangement based on the idea of a virtual microphone that can "project" the zone of quiet so that it is further away from the secondary source than the physical error microphone. Experimental validation of this arrangement has shown that this sort of arrangement is suitable for practical applications such as a local active noise control system in a headrest up to frequencies of about 500 Hz [7, 14].

Figure 18 shows the block diagram of a single channel virtual microphone arrangement using a two-loudspeaker secondary source array to cancel the acoustic pressure at a virtual microphone position, (v), and the second particle velocity, u_s, at a different field point located between the physical and the virtual microphone positions. The block diagram shows that the total pressure at the virtual microphone position is estimated from the measured pressure at the physical microphone position, (a), and the knowledge of the acoustic transfer

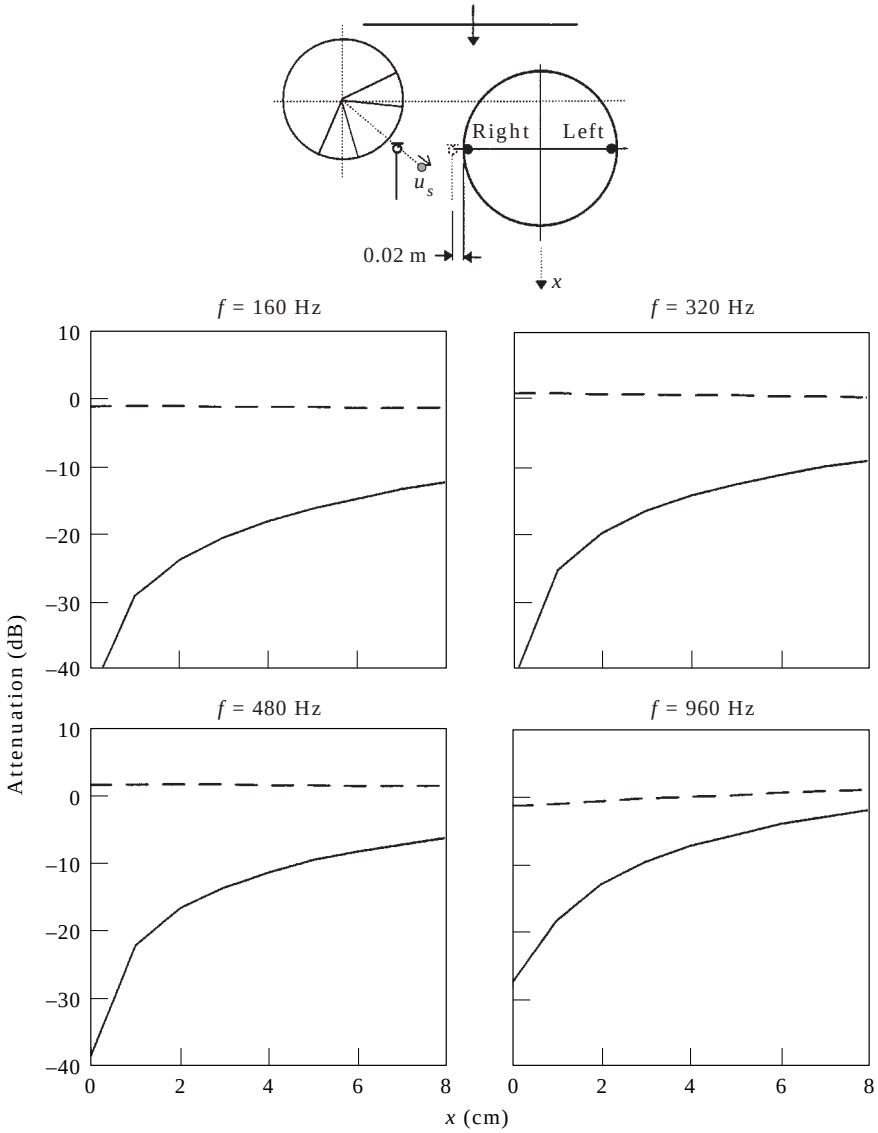

Figure 23. The calculated controlled acoustic field at the measuring points corresponding to the right (continuous) and left (dashed line) hand ears of the listener (black dots) when the secondary spherical source with an active segment and a ring seeks to cancel the primary acoustic field at a virtual microphone position and the on-axis secondary particle velocity component at a point in the near field, for different positions of the rigid sphere along the x-axis. The primary acoustic field is a plane propagating in the positive x-direction. $y = 0$, $z = 0$.

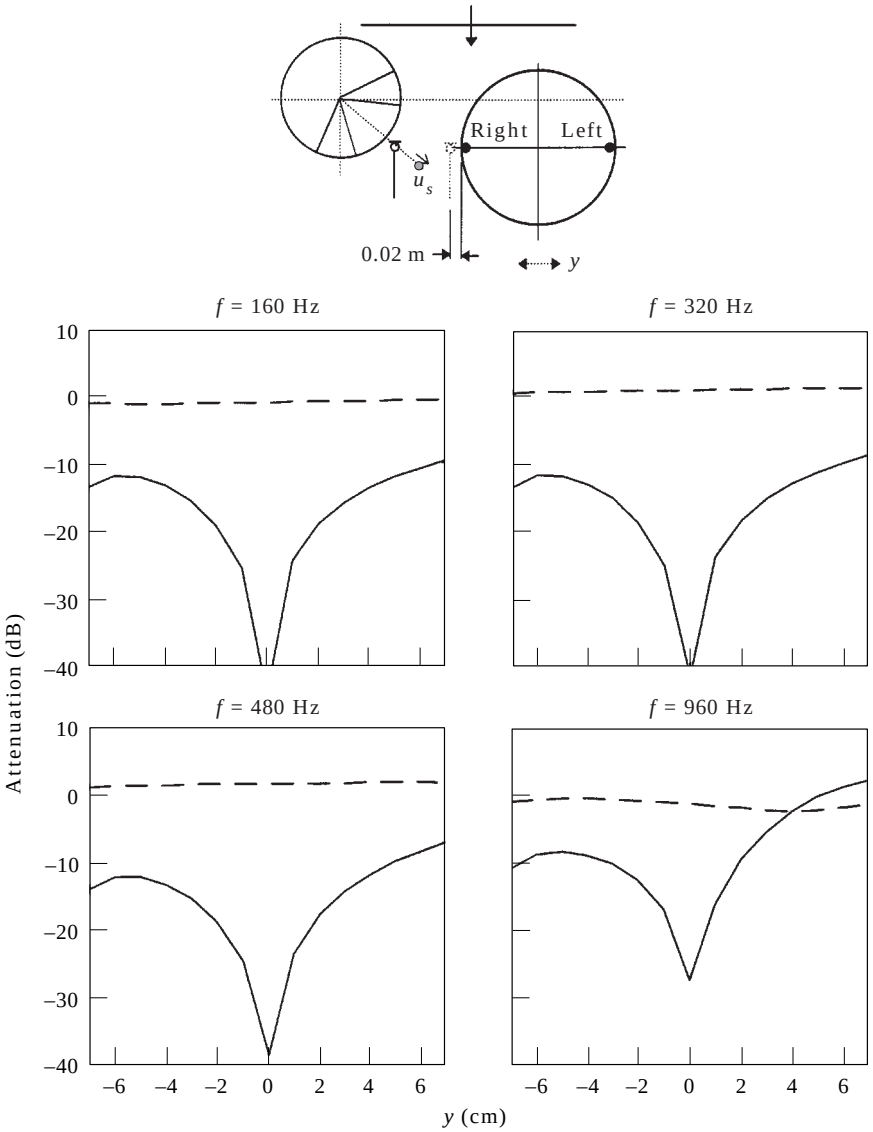

Figure 24. The calculated controlled acoustic field at the measuring points corresponding to the right (continuous) and left (dashed line) hand ears of the listener (black dots) when the secondary spherical source with an active segment and a ring seeks to cancel the primary acoustic field at a virtual microphone position and the on-axis secondary particle velocity component at a point in the near field, for different positions of the rigid sphere along the y-axis. The primary acoustic field is a plane propagating in the positive x-direction. $x = 0$, $z = 0$.

impedances from the source array to the physical and the virtual microphone positions, i.e., Z_a and Z_v. In this type of arrangement, the primary sound field at the physical and virtual microphone positions is assumed to be the same, which is reasonable if the distance between these two positions is small compared with the acoustic wavelength, since the two microphones are in the far field of the primary source. Thus, upon knowing Z_a, Z_v and the electrical input to the source array, q, the output from the physical microphone (a) can be electrically processed,

as illustrated in Figure 18, to give $\hat{p}_v$ which can be driven to zero by the control system, thus producing a zone of quiet around the virtual microphone location. One can note that, for a single frequency excitation, the cancellation of the secondary particle velocity component in a particular direction at a field point can always be achieved by implementing a suitable filter with a transfer function H (see Figure 18) which can be defined experimentally from the measurements of the

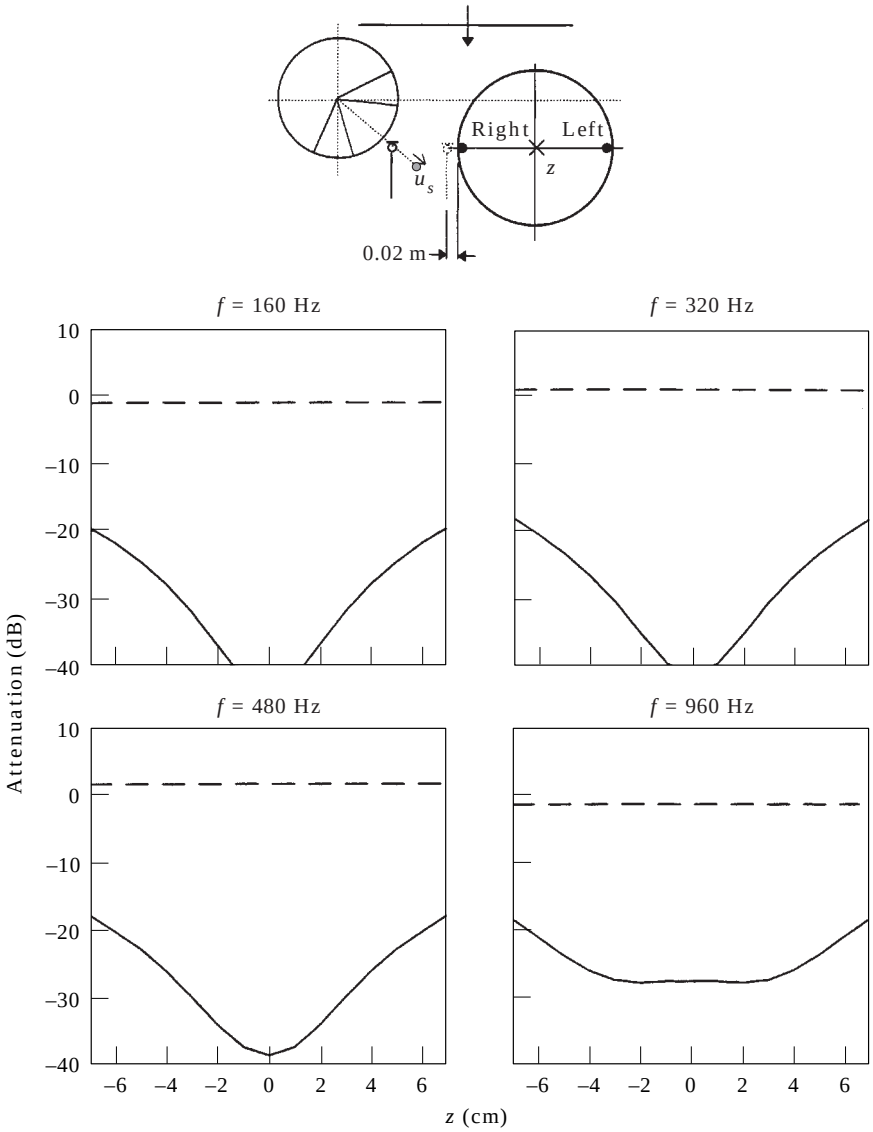

Figure 25. The calculated controlled acoustic field at the measuring points corresponding to the right (continuous) and left (dashed line) hand ears of the listener (black dots) when the secondary spherical source with an active segment and a ring seeks to cancel the primary acoustic field at a virtual microphone position and the on-axis secondary particle velocity component at a point in the near field, for different positions of the rigid sphere along the z-axis. The primary acoustic field is a plane propagating in the positive x-direction. $x = 0$, $y = 0$.

particle velocity component produced independently by each loudspeaker in the source array.

Since concern here is mainly with the generation of zones of quiet in a relatively low frequency range, say up to 1 kHz, the actual geometric details of the local active noise control arrangement may be neglected and one can assume that for a particular error microphone location, the generation of the near field zone of quiet is mainly dictated by the relative size and proximity of the secondary source and the diffracting sphere. Under this assumption, the two-sphere model described in the previous section can be used to predict the attenuation at the listener's ears in a practical local active noise control system [14].

Figure 19 shows the simple model used here to predict the zone of quiet created when a two-loudspeaker source in an active headrest, for example (modelled as a spherical source of radius 0·08 m with an active segment of 50° and a ring of maximum angle 120°) seeks to cancel the pressure at a virtual microphone location near a diffracting head and the secondary velocity component at a point on-axis and at a distance of 0·05 m from the source. The diffracting head has been modelled as a rigid sphere of radius 0·115 m which approximates the mean radius of a human head. To be consistent with previous work [14], the axis of the active segment in the model of Figure 19 forms an angle of $-25°$ with the y-axis. In the simulations reported next the primary field is considered to be a plane wave propagating in the positive x-direction (see Figure 19) instead of a diffuse sound field. This allows a simplification of the simulations, which otherwise would be very time consuming, and is consistent with previous theoretical and experimental work reported in references [7] and [14]. However, it can be anticipated that in the frequency range of use of a practical local active noise control system, say below 500 Hz, the extents of the achievable zone of quiet in both types of primary sound fields are similar [15].

Figures 20–22 show the calculated attenuation at the right-hand (continuous) and left-hand (dashed line) ears when the secondary spherical source with an active segment of 120° seeks to cancel the pressure at the virtual microphone position for different displacements of the rigid sphere in the x, y and z directions, respectively, as defined in Figure 19. These results show how the attenuation at the ears changes for different positions of the diffracting sphere along the x, y and z axes. The predictions shown correspond to four different values of the excitation frequency, i.e., 160, 320, 480 and 960 Hz. These frequency values were chosen to be consistent with the measurements reported in previous work [7, 14]. The attenuation curves of Figures 20–22 can be compared with the results shown in Figures 23–25 which depict the calculated attenuation at the listener's ears when the secondary spherical source with an active segment and a ring, as defined in Figure 19, cancels the primary pressure at the virtual microphone position and the secondary particle velocity in the axial direction at a point on-axis located at 0·05 m from the source. These results suggest that a two-loudspeaker source array used in a virtual microphone arrangement as shown in Figure 18 can potentially produce high sound reductions at the listener's ears. Comparing the results in Figures 20–22 with those in Figures 23–25, respectively, suggests that the simultaneous cancellation of pressure and secondary particle velocity in the near

field of a source radiating near a diffracting head in a local active noise control system can provide a considerable improvement in the extent of the zones of quiet along the three directions of the co-ordinate axis.

8. CONCLUSIONS

The control strategy of cancelling the acoustic pressure and the particle velocity component at a point in the near field of a secondary source array seems to offer new possibilities to improve the acoustic performance of a local active noise control system. For most local active noise control systems the spatial rate of change (gradient) of the primary acoustic field near the cancellation point is small compared with that of the secondary field. Under these circumstances, the strategy of controlling the pressure and the *total* particle velocity in the near field of the secondary source gives similar results to controlling the pressure and the *secondary* particle velocity component instead.

The acoustic performance of a local active noise control system which cancels the pressure at a virtual microphone position near a diffracting head and the secondary particle velocity at an intermediate point between the secondary source and the diffracting sphere has also been explored. This strategy avoids having to drive the active parts of the secondary source array very hard to achieve secondary velocity component cancellation and, at the same time, produces a considerable improvement in the extent of the zones of quiet with respect to the case of cancelling the acoustic pressure only.

REFERENCES

1. S. J. Elliott and J. Garcia-Bonito 1995 *Journal of Sound and Vibration* **186**, 696–704. Active cancellation of pressure and pressure gradient in a diffuse sound field.
2. M. Miyoshi, J. Shimizu and N. Koizumi 1994 *Inter-noise* **94**, 1299–1304. On arrangements of noise controlled points for producing larger quiet zones with multi-point active noise control.
3. S. Ise 1994 *Inter-noise* **94**, 1339–1342. Theory of acoustic impedance control for active noise control.
4. J. Garcia-Bonito and S. J. Elliott 1994 *Institute of Sound and Vibration*, *Technical Memorandum* 745. Alternative strategies for actively generated quiet zones.
5. A. David and S. J. Elliott 1994 *Applied Acoustics* **41**, 63–79. Numerical studies of actively generated quiet zones.
6. J. Garcia-Bonito and S. J. Elliott 1995 *Journal of the Acoustical Society of America* **98**, 1017–1024. Local active control of diffracted diffuse sound fields.
7. J. Garcia-Bonito, S. J. Elliott and C. C. Boucher 1996 *Inter-noise* **96**, 1115–1120. A virtual microphone arrangement in a practical active headrest.
8. F. Jacobsen 1979 *The Acoustics Laboratory*. *Technical University of Denmark*. *Report No*. 27. The diffuse sound field.
9. L. E. Kinsler, A. R. Frey, A. B. Coppens and J. V. Sanders 1982 *Fundamental of Acoustics*. New York: Wiley; second edition.
10. I. Malecki 1969 *Physical Foundations of Technical Acoustics*. Oxford: Pergamon Press; first edition.
11. P. M. Morse 1948 *Vibration and Sound*. New York: McGraw-Hill.
12. P. Joseph, S. J. Elliott and P. A. Nelson 1994 *Journal of Sound and Vibration* **172**, 605–627. Near field zones of quiet.

13. S. J. ELLIOTT and A. DAVID 1992 1*st International Conference on Motion and Vibration Control*, *Yokohama*. A virtual microphone arrangement for local active sound control.
14. J. GARCIA-BONITO, S. J. ELLIOTT and C. C. BOUCHER 1997 *Journal of the Acoustical Society of America* **101**, 3498–3516. Generation of zones of quiet using a virtual microphone arrangement.
15. J. GARCIA-BONITO 1996 *PhD. Thesis*, *Institute of Sound and Vibration Research*, *University of Southampton*, *England*. Local active control in pure tone diffracted diffuse sound fields.